Published in final edited form as:
Neuropharmacology. 2014 November ; 86: 228–240. doi:10.1016/j.neuropharm.2014.07.016.

Salvinorin A Regulates Dopamine Transporter Function Via A Kappa Opioid Receptor and ERK1/2-Dependent Mechanism

Bronwyn Kivell[a,d,#], **Zeljko Uzelac**[b,#], **Santhanalakshmi Sundaramurthy**[c], **Jeyaganesh Rajamanickam**[c], **Amy Ewald**[a], **Vladimir Chefer**[d], **Vanaja Jaligam**[d], **Elizabeth Bolan**[d], **Bridget Simonson**[a], **Balasubramaniam Annamalai**[e], **Padmanabhan Mannangatti**[c], **Thomas Prisinzano**[f], **Ivone Gomes**[g], **Lakshmi A. Devi**[g], **Lankupalle D. Jayanthi**[c], **Harald H. Sitte**[b,§], **Sammanda Ramamoorthy**[c,§,*], and **Toni S. Shippenberg**[d,§]

[a]School of Biological Sciences, Victoria University of Wellington, Wellington, New Zealand [b]Medical University Vienna, Center for Physiology and Pharmacology, Institute of Pharmacology, Waehringerstrasse 13a, A-1090 Vienna, Austria (Z.U., H.H.S.) [c]Department of Pharmacology and Toxicology, Virginia Commonwealth University, Richmond, VA 23298, USA [d]Integrative Neuroscience Section, National Institutes of Health, National Institute on Drug Abuse Intramural Research Program, Baltimore MD 21224, USA [e]Department of Neurosciences, Medical University of South Carolina, Charleston SC, 29425, USA [f]Department of Medicinal Chemistry, University of Kansas, Lawrence, Kansas, 66045, USA [g]Department of Pharmacology and Systems Therapeutics, Mount Sinai School of Medicine, New York, NY 10029, USA

Abstract

Salvinorin A (SalA), a selective κ-opioid receptor (KOR) agonist, produces dysphoria and pro-depressant like effects. These actions have been attributed to inhibition of striatal dopamine release. The dopamine transporter (DAT) regulates dopamine transmission via uptake of released neurotransmitter. KORs are apposed to DAT in dopamine nerve terminals suggesting an additional target by which SalA modulates dopamine transmission. SalA produced a concentration-dependent, nor-binaltorphimine (BNI)- and pertussis toxin-sensitive increase of ASP^+ accumulation in EM4 cells coexpressing myc-KOR and YFP-DAT, using live cell imaging and

[*]Corresponding author: Sammanda Ramamoorthy, Ph.D., Department of Pharmacology and Toxicology, Virginia Commonwealth University, R. Blackwell Smith Building, Room # 756A, 410 North, 12th Street, Richmond, VA 23298, sramamoorthy@vcu.edu, Phone: 804-828-8407, Fax: 804-828-2117.
[#]B.K., Z.U. contributed equally to this work.
[§]H.H.S., S.R., T.S.S. contributed equally to this work.

Authorship Contributions: *Participated in research design:* Kivell, B., Chefer, V., Devi, L.A., Jayanthi, L.D., Sitte, H.H., Ramamoorthy, S, Shippenberg, T.S.
Conducted experiments: Kivell, B., Chefer, V., Jaligam, V., Bolan, E., Simonson, B., Sundaramurthy, S., Rajamanickam, J., Ewald, A., Annamalai, B., Mannangatti, P., Gomes, I. Uzelac, Z.
Contributed new reagents or analytic tools: Prisinzano, T.
Performed data analysis: Kivell, B., Chefer, V., Gomes, I, Devi, L.A., Sitte, H.H., Ramamoorthy, S, Shippenberg, T.S.
Wrote or contributed to the writing of the manuscript: Kivell, B., Chefer, V., Sitte, H.H., Ramamoorthy, S, Shippenberg, T.S

the fluorescent monoamine transporter substrate, trans 4-(4-(dimethylamino)-styryl)-N-methylpyridinium) (ASP^+). Other KOR agonists also increased DAT activity that was abolished by BNI pretreatment. While SalA increased DAT activity, SalA treatment decreased serotonin transporter (SERT) activity and had no effect on norepinephrine transporter (NET) activity. In striatum, SalA increased the V_{max} for DAT mediated DA transport and DAT surface expression. SalA up-regulation of DAT function is mediated by KOR activation and the KOR-linked extracellular signal regulated kinase-½ (ERK1/2) pathway. Co-immunoprecipitation and BRET studies revealed that DAT and KOR exist in a complex. In live cells, DAT and KOR exhibited robust FRET signals under basal conditions. SalA exposure caused a rapid and significant increase of the FRET signal. This suggests that the formation of KOR and DAT complexes is promoted in response to KOR activation. Together, these data suggest that enhanced DA transport and decreased DA release resulting in decreased dopamine signaling may contribute to the dysphoric and pro-depressant like effects of SalA and other KOR agonists.

Keywords

kappa opioid receptor; dysphoric; pro-depressant; dopamine transporter; serotonin transporter; trafficking; salvinorin A

1. Introduction

Salvinorin A (SalA) is a naturally occurring κ-opioid receptor (KOR) agonist that produces psychotomimesis, dysphoria and prodepressant like effects (Vortherms and Roth, 2006). Despite a surge in its recreational use (Griffin et al., 2008), the neural correlates mediating these effects are unknown. Decreased dopamine signaling in the dorsal and ventral striatum is implicated in the induction of dysphoria and the pathogenesis of depression (Mizrahi et al., 2007). KOR agonists decrease dopamine concentrations in these regions; an effect attributed to inhibition of dopamine release (Shippenberg et al., 2007; Spanagel et al., 1990).

The dopamine transporter (DAT) rapidly clears the dopamine released into the extracellular space and the activity of DAT is the determinant of dopamine signaling (Amara and Kuhar, 1993). It is largely evident that DAT activity is rapidly altered in response to activation and or inhibition of several protein kinases and protein phosphatase PP1/PP2Ac. For example, activation of PKC as well as inhibition of ERK1/2, PI-3 kinase, CaMKII, Cdk5 and tyrosine kinase rapidly decrease DA uptake (Carvelli et al., 2002; Doolen and Zahniser, 2001; Fog et al., 2006; Moron et al., 2003; Price et al., 2009; Zhang et al., 1997). In addition, while activation of D2, D3 DA receptors ($D_{2s}R$, D_3R), TrkB and insulin receptors stimulates DA uptake, activation of NK1R or mGluR5 reduces DA uptake (Bolan et al., 2007; Garcia et al., 2005; Granas et al., 2003; Hoover et al., 2007; Lee et al., 2007; Mayfield and Zahniser, 2001; Page et al., 2001; Zapata et al., 2007). Thus, G-protein coupled receptor (GPCR) and non-GPCR receptor regulation of DAT has been well documented (reviewed and references therein (Ramamoorthy et al., 2011)). The contributions of regulated DAT phosphorylation (Khoshbouei et al., 2004), ubiquitylation (Miranda et al., 2005), palmitoylation (Foster and Vaughan, 2011), glycosylation (Li et al., 2004), protein-protein interaction (reviewed (Eriksen et al., 2010)-therein references) and lipid-raft distribution (Adkins et al., 2007) have been demonstrated in regulating DAT-trafficking, DAT-mediated DA-efflux and

degradation. Furthermore, DAT-substrates and inhibitors can also influence kinase/phosphatase mediated DAT regulation (Melikian, 2004; Pramod et al., 2013; Ramamoorthy et al., 2011; Vaughan and Foster, 2013).

KOR is apposed to DAT in striatal dopamine axons and varicosities (Svingos et al., 2001). These findings indicate that KOR is strategically located to regulate dopamine uptake and that DAT may be a target upon which SalA acts to modulate dopamine transmission and behavior. However, our knowledge of the SalA mediated KOR-signaling mechanisms that contribute to DAT regulation is incomplete. The present studies, conducted in heterologous expression systems and native tissue, examined whether SalA modulates DAT function and the intracellular mechanisms mediating this effect.

2. Materials and Methods

2.1. Live Cell Imaging to Quantify DAT function

Experiments were conducted in HEK-293 (HEK) and EM4 cells, a HEK cell line expressing a macrophage scavenger receptor to increase adherence to tissue culture plastic. Cells were maintained in DMEM/Ham's F-12 medium (50:50; Mediatech Inc., Herndon, VA) supplemented with 10% FBS and grown in a humidified atmosphere (37°C and 5% CO_2). Cells were transfected with myc-rat KOR (KOR; 0.1 μg) and either 0.3 μg of YFP-human DAT (DAT), eGFP-rat DAT (rDAT), FLAG-human DAT (FLAG-DAT) or GFP-human norepinephrine transporter (NET), or human serotonin transporter (hSERT) 24 h after plating, using Lipofectamine™ LTX (Invitrogen, Carlsbad, CA). Experiments were performed 48 h later (cell confluency: 70-80%). Addition of these tags does not alter the trafficking, protein localization or function (Jordan and Devi, 1999; Zapata et al., 2007).

Time-resolved quantification of DAT function in single cells was achieved using the fluorescent, high affinity monoamine transporter substrate 4-(4-diethylaminostyryl)-*N*-methylpyridinium iodide (ASP^+) (Schwartz et al., 2003). ASP^+ is a sensitive probe for monitoring monoamine transporter function (Bolan et al., 2007; Schwartz et al., 2003; Zapata et al., 2007). ASP^+ accumulation is linear for 10 min after ASP^+ addition, inhibited by substrates and dependent on temperature and extracellular NaCl concentrations. Immediately before experiments, media was removed and cells washed in Krebs-Ringer/HEPES medium (KRH in mM: 130 NaCl, 1.3 KCl, 2.2 $CaCl_2$, 1.2 $MgS0_4$, 1.2 KH_2PO_4, 10 HEPES, and 1.8 g/liter glucose, pH 7.4). Fresh KRH was added, and the culture dish was mounted on an Ultra VIEW™ LCI spinning-disk (PerkinElmer Life Sciences (Grand Island, NY) or Olympus FV1000 (Olympus, Tokyo, Japan) confocal microscope (60x water objective lens). A within cell design was used to assess the effects of graded SalA concentrations (0.1-10 μM), and to determine ASP^+ uptake kinetics. The microscope was focused on a cell monolayer and background auto-fluorescence determined by collecting an image immediately prior to replacing buffer with that containing ASP^+ (10 μM). SalA, SalA, U69,593 or U50,488 or vehicle was added 5 min later. The slope of ASP^+ accumulation was determined before and after addition. Images were collected every 20 s for 10 min to capture YFP or GFP (excitation, 488 nm; emission, 525–575 nm) and ASP^+ fluorescence (excitation, 488 nm; emission, 607–652 nm). To determine ASP^+ uptake kinetics, a range of ASP^+ concentrations (0-16 μM) were used. The slope of uptake phase was determined

following background subtraction (cells not expressing DAT) and normalization to cell surface expression of either DAT or SERT. For studies assessing the effects of the selective KOR antagonist, nor-binaltorphimine (BNI: 1 μM; 10 min), pertussis toxin (PTX: 100 ng/ml; 16-24 hr) or the selective extracellular signal regulated kinase 1/2 (ERK) inhibitor, PD98059 (10 μM; 15 min) or p38 MAP kinase inhibitor SB203580 (3 μM; 5 min) (Tocris; Minneapolis, MN) or dopamine D_2 receptor antagonist L-741,626 (10 μM; 5 min) (Tocris; Minneapolis, MN) on SalA-evoked alterations of ASP^+ uptake, cells were incubated with drug for the indicated times and the slope of ASP^+ accumulation quantified as above. Drug concentrations were chosen based on reported effective concentrations (Alessi et al., 1995; Bolan et al., 2007; Dalman and O'Malley, 1999; Grilli et al., 2009; Zapata et al., 2007). Fluorescent images were processed using Velocity (PerkinElmer Life Sciences) and NIH ImageJ (version 1.32) software. Within cell fluorescent accumulation, defined by GFP or YFP plasma membrane fluorescence, was measured as average pixel intensity of time-resolved images. Data are expressed as arbitrary fluorescence units (AFU) or percent change in ASP^+ uptake rate after drug addition. Typically 30–100 cells from three separate transfections were used.

2.2. Quantification of Striatal DAT Function

All Procedures with rodents were approved by the Institutional Animal Care and Use Committee in accordance with the National Institutes of Health Guide (NIH Publication No. 8023, revised 1978) for the Care and Use of Laboratory Animals and the Victoria University of Wellington Animal Ethics Committee. Rats were maintained in a temperature and humidity controlled room on a 12:12 h light/dark cycle. Food and water were supplied *ad* libitum. All efforts and care were taken to minimize animal suffering and to reduce the number of animals used. As alternatives to brain tissues, cell culture models were utilized.

2.2.1. Rotating Disk Electrode (RDE) Voltammetry—RDE was used to determine the initial velocity of dopamine clearance in minces of the striatal tissue of rats as previously described using an electrode rotation rate of 4000 rpm and an applied potential of +450 mV versus Ag/AgCl reference electrode (Thompson et al., 2000). Voltage output was monitored until stable baselines were obtained (≈10 min). SalA or U50,488 (3 μl; final cell concentration: 10 nM) or an equivalent volume of vehicle was added to the electrochemical cell 4-5 min prior to addition of dopamine (6 μl; final concentration: 2 μM). PD98050 (3 μl; final concentration: 10 μM) was added to the cell, followed 10 min later by SalA. The resultant signals were detected as changes in voltage output versus time using electrochemical detection. The initial rate of signal decay after dopamine addition was calculated for 10 s. Rates of nonspecific signal decay, defined as signal decay in the absence of tissue at the end of each experimental day, were subtracted from that in the presence of tissue to calculate initial velocity of DA clearance (pmoles/s/g wet weight tissue). DA-clearance in the presence of GBR12909 was subtracted from DA clearance in absence of GBR12909 to derive DAT-mediated DA clearance..

2.2.2. [^{3}H]DA uptake assay—Synaptosomes from striatum were prepared and [^{3}H]DA uptake was measured as described previously (Tejeda et al., 2013). Briefly, rats were rapidly decapitated, and striatal regions were dissected and collected in 10 volumes (wt/vol) of cold

0.32 M sucrose. The tissue was immediately homogenized using a Teflon-glass homogenizer and centrifuged at 1000 × g for 15 min at 4°C. The resulting supernatant was centrifuged at 12,000 × g for 20 min and the pellet was washed by resuspending in 0.32 M sucrose. The synaptosomal preparation was used immediately for experiments. Protein concentration was determined by DC protein assay (BioRad) using bovine serum albumin as standard. Striatal synaptosomes (40 μg) were incubated in a total volume of 0.5 ml of Krebs-Ringer-HEPES (KRH) buffer consisting of 120 mM NaCl, 4.7 mM KCl, 2.2 mM $CaCl_2$ 10 mM HEPES, 1.2 mM $MgSO_4$, 1.2 mM KH_2PO_4, 5 mM Tris, 10 mM D- glucose, pH 7.4 containing 0.1 mM ascorbic acid, and 0.1 mM pargyline in the presence of SalA (10 μM) or appropriate vehicle at 37°C for 5 min. Uptake was initiated by the addition of 10 nM [^{3}H]DA (78 Ci/mmoldihydroxyphenylethylamine [2,5,6,7,8-^{3}H], PerkinElmer, Santa Clara, CA). Unlabelled DA was used along with [^{3}H]DA from 0.01 nM to 2.0 μM for saturation analysis. Uptake was terminated with the addition of 3 ml ice-cold PBS followed by rapid filtration over 0.3% polyethylenimine coated GF-B filters on a Brandel Cell Harvester (Brandel Inc., Gaithersburg, MD). Filters were washed rapidly with 5 ml cold PBS and radioactivity bound to filter was counted by liquid scintillation counter. Nonspecific uptake, defined as the uptake in the presence of 100 μM cocaine, was subtracted from total accumulation of [^{3}H]DA to yield specific total DA uptake (representing DA uptake mediated by both DAT and NET). To isolate only DAT-mediated [^{3}H]DA uptake from total [^{3}H]DA uptake (DAT/NET-specific), NET-specific blocker nisoxetine (50 nM) was used to block NET-mediated DA transport as described earlier (Tejeda et al., 2013). DAT specific DA uptake was further verified using specific DAT blocker GBR12909 (50 nM) or nomifensine (100 nM). DAT activity isolated in this manner was completely blocked by DAT blockers GB12909 or nomifensine. Thus, [^{3}H]DA uptake in the presence of nisoxetine corresponds to specific DA uptake through DAT. All uptake assays were performed in triplicates and expressed as mean values of specific uptake ± S.E.M.

2.3. Immunoblotting of ERK1/2 and p38 MAPK

Immunoblotting of phosphorylated ERK (p-ERK) and p38 MAPK (phospho-p38 MAPK) were conducted in EM4 cells that are serum-starved for 2 h. Cells were incubated with SalA (10 μM) or vehicle for 5 min at 37 °C. PD98059 (10 μM) was preincubated for 15 min prior to SalA addition. Following the treatment, the media was aspirated and the cells were washed before solubilizing with RIPA buffer (10 mM Tris-HCl, pH 7.5, 150 mM NaCl, 1 mM EDTA, 1% Triton X-100, 0.1% SDS, and 1% sodium deoxycholate) supplemented with a cocktail of protease and phosphatase inhibitors. Equal amount of protein was incubated with Laemmli buffer (62.5 mM Tris, pH 6.8, 20% glycerol, 2% SDS, 5% β-mercaptoethanol, and 0.01% bromphenol blue) and proteins separated by SDS-PAGE and transferred onto polyvinylidene difluoride membranes (Millipore, Bellerica, MA). Membranes were blocked for 1 h at room temperature in TBS-T containing 5% nonfat milk. p-ERK and phospho-p38 MAPK were detected using rabbit polyclonal antibody specific for p44/42 MAPK phosphorylated at threonine 202 and tyrosine 204 and threonine 180 and tyrosine 182 respectively. To analyze total ERK and p38 MAPK levels, blots were stripped with 2% SDS and 100 mM β-mercaptoethanol in 62.5 mM Tris, pH 6.8, for 1 h at 50 °C and reprobed with polyclonal antibodies (Cell Signaling Technology, Inc. Beverly, MA) recognizing total ERK or total p38 MAPK. Blots were visualized using HRP-conjugated

secondary antibody (Jackson ImmunoResearch Laboratories, West Grove, PA) with enhanced chemiluminescence reagents (Amersham Biosciences, GE healthcare, NJ). Multiple exposures were evaluated by digital quantitation using NIH ImageJ (version 1.32j) software to ensure that results were within the linear range of film exposure. Amounts of p-ERK and phospho-p38 MAPK were normalized to that of total ERK and total p38 MAPK respectively (Bolan et al., 2007).

2.4. Cell Surface Biotinylation and Immunoblotting

Cell surface biotinylation and immunoblotting was performed as described previously (Zapata et al., 2007). *Cells:* Briefly, EM4 cells (100,000 cells/well) transfected with myc-KOR and FLAG-DAT were grown in 12 well plates were first washed PBS/Ca-Mg (138 mM NaCl, 2.7 mM KCl, 1.5 mM KH_2PO_4, 9.6 mM Na_2HPO_4, 1 mM $MgCl_2$, 0.1 mM $CaCl_2$, pH 7.3). Where indicated, cells were treated with different modulators at 37°C as described in figure legends. Then cells were incubated with EZ link NHS-Sulfo-SS-biotin (1 mg/ml) (Thermo Fisher Scientific, Rockford, IL) in cold PBS/Ca-Mg for 30 min on ice and then the excess biotinylating reagents were removed by two times wash with 100 mM glycine and further incubated with glycine for 20 min. The cells were solubilized using RIPA buffer supplemented with a cocktail of protease inhibitors. *Synaptosomes:* Briefly, Synaptosomes (300 to 500 μg) were incubated in Krebs-Ringer buffer with indicated modulators or vehicle at 37°C for the times indicated in figure legends (Samuvel et al., 2008). The samples were washed quickly by centrifugation, and the pellets were treated with EZ link NHS-Sulfo-SS-biotin (1 mg/1 mg protein) for 30 min at 4°C in in cold Krebs-bicarbonate buffer. Subsequently, the samples were washed with the same buffer containing 100 mM glycine, and the pellet was resuspended in RIPA lysis buffer. The resuspended synaptosomes or solubilized cells were triturated 10 times through a 25 gauge needle and centrifuged at 25,000 × g for 30 min. Total cellular protein content was determined by the Bradford Protein Assay procedure. Using equal amounts of solubilized proteins, the biotinylated proteins were isolated using NeutrAvidin Agarose resins overnight at 4°C followed by washing. Bound proteins were eluted with 50 μl Laemmli sample buffer for 30 min at room temperature. Aliquots from total extracts, unbound fractions and all of the eluate were separated by SDS-PAGE, transferred to polyvinylidene difluoride membrane and probed with DAT specific (Santa Cruz Biotechnology, Inc. Dallas, TX) or other antibodies as indicated. The immunoreactive proteins were visualized using ECL or ECL plus reagent. Subsequently, the blots were stripped and reprobed with anti-calnexin antibody (AKELA Pharma Inc. Montreal, QC, Canada) to validate the surface biotinylation of plasma membrane proteins as well as protein loading levels. DAT densities from total and biotinylated (representing the surface pool) fractions were normalized using levels of calnexin in the total extract. Multiple exposures were evaluated by digital quantitation using NIH ImageJ (version 1.32j) software to ensure that results were within the linear range of the film exposure (Samuvel et al., 2008; Zapata et al., 2007).

2.5. Identification of DAT-KOR Complexes

2.5.1. Co-immunoprecipitation and Immunoblot Analysis—Co-immunoprecipitation experiments were conducted using EM4 cells or striatal synaptosomes. *A. EM4 cells:* Co-immunoprecipitation experiments were conducted as previously described

(Bolan et al., 2007) in EM4 cells expressing myc-KOR and FLAG-DAT alone or together. Protein samples were prepared by incubation of cells with RIPA buffer pH 7.4, for 30 min (4°C) followed by centrifugation (25,000 × g for 30 min). Complexes were immunoprecipitated with polyclonal anti-myc antibodies (rabbit, clone A-14, Santa Cruz Biotechnology, CA). After pull down with Protein A-linked agarose beads, they were washed three times with RIPA buffer and eluted at room temperature. Immunoprecipitates were separated by SDS-PAGE (4-20% Duramide gradient gel, Cambrex, Walkersville, MD) and blotted onto polyvinylidene difluoride membranes. DAT was detected using a monoclonal antibody raised against the N-terminal domain of human DAT (Chemicon, Temecula, CA) and secondary goat HRP-conjugated anti-rat antibody (Jackson ImmunoResearch, West Grove, PA). *B. Striatal synaptosomes*. Presence of KOR protein in immunoprecipitated DAT protein complex. Immunoprecipitation of DAT protein was carried out using two DAT antibodies from Chemicon (Millipore), Billerica, MA and Santa Cruz Biotechnology, Inc. Dellas, TX as described (Chakrabarti et al., 2010). Synaptosomes (500-700 μg) were solubilized with 20 mM Hepes buffer, pH 7.4 containing 150 mM NaCl, 5 mM EDTA, 1% Triton X-100, 0.1% SDS supplemented with a cocktail of protease and phosphatase inhibitors. In parallel, irrelevant IgG was used as a control. Clear solubilized extract after centrifugation (25,000 g for 45 min) was incubated with DAT antibodies (4 μg) overnight at 4°C, and the immunocomplex was isolated using Protein A and G Sepharose. Immunoprecipitates eluted with Laemmli buffer with out β-mercaptoethanol. The eluted samples were then incubated with 5% β-mercaptoethanol, and 0.01% bromphenol blue for 30 min at 22°C, electrophoresed as given above. The presence of KOR protein from DAT-immunocomplex was detected by immunoblotting using rabbit polyclonal KOR-1 antibody (Santa Cruz Biotechnology, Inc. Dellas, TX).

2.5.2. Biolumiescence Resonance Energy Transfer (BRET)—BRET studies were carried out with HEK cells transfected with luciferase tagged KOR (Luc-KOR) alone or with YFP-DAT as described previously using a FluoroMax-2 spectrometer and the Fusion Microplate Reader (Bolan et al., 2007). BRET ratios were calculated as described by Angers et al., (2000) (Angers et al., 2000). Cells transfected with Luc-KOR in combination with YFP-tagged delta opioid receptor (YFP-DOR) were used as a positive control since studies have shown that KOR and DOR functionally interact and are in close proximity (Gomes et al., 2003). As a negative control, we used cells co-transfected with YFP-tagged chemokine receptors CCR5 (YFP-CCR5) and Luc-KOR.

2.5.3. Fluorescence Resonance Energy Transfer (FRET)—FRET (Schmid and Sitte, 2003) was measured with a Carl Zeiss Axiovert 200 epifluorescence microscope. The ‘three-filter method’ was performed as described in (Bartholomaus et al., 2008). Images were taken using 63x oil immersion objectives and LUDL filter wheels allowing a rapid excitation and emission filter exchange. We used HEK293 cells which were maintained and transiently transfected with plasmid cDNA (1.7 μg) by means of the calcium phosphate co-precipitation method as described previously (Sucic et al., 2010). The LUDL filter wheels were configured as follows: CFP (I_{Donor}; excitation: 436nm, emission: 480nm, and dichroic mirror: 455nm), YFP ($I_{Acceptor}$; excitation: 500nm, emission: 535nm, and dichroic mirror: 515nm) and FRET (I_{FRET}; excitation: 436nm, emission: 535nm, and dichroic mirror:

455nm). Images were taken with a CCD camera (Coolsnap *fx*, Roper Scientific). Background fluorescence was subtracted from all images. We analyzed the images pixel by pixel using ImageJ (Wayne Rassband, National Institute of Health, version 1.43b) and the ImageJ plug-in PixFRET (Pixel by Pixel analysis of FRET with ImageJ, version 1.5.0; Feige et al., 2003) with which spectral bleed-through (SBT) parameters for the donor bleed through (BT) and the acceptor BT were determined and NFRET was calculated in the following way:

$$\mathrm{nFRET}=\frac{\mathrm{IFRET}-\mathrm{BTDonor}*\mathrm{IDonor}-\mathrm{BTAcceptor}*\mathrm{IAcceptor}}{\sqrt{\mathrm{IDonor}*\mathrm{IAcceptor}}}*100$$

The mean N_{FRET} was measured at the plasma membrane (pre-defined as the *region of interest*) using the computed N_{FRET}-image. The regions of interest were selected in the CFP (Donor) or YFP (Acceptor) image (to avoid bleaching-associated bias) and transmitted to the N_{FRET}-image by the ImageJ Multi Measure Tool. As negative control we employed the YFP-labeled form of KOR with a membrane-bound form of CFP (kindly provided by R.Y. Tsien). As positive controls for membrane proteins we used the SERT tagged with CFP and YFP on its cytoplasmic N- and C-termini, respectively (to yield C-SERT-Y; (Just et al., 2004)). We tagged DAT and GAT1 with CFP to reveal C-DAT and C-GAT1 (Schmid et al., 2001) to compare the FRET values between Y-KOR and C-DAT or C-GAT1. To compare expression levels of CFP- or YFP-tagged proteins, the fluorescence intensity within a rim of a few pixels positioned over the membrane was measured and expressed in arbitrary fluorescence units (a.f.u.).

2.6. Purification of SalA

SalA was isolated and purified from commercially available *Salvia divinorum* leaves as described previously (Butelman et al., 2007; Tidgewell et al., 2004) and determined to be >98% pure by HPLC.

2.7. Statistical Analysis

Values are expressed as mean ± S.E.M. As noted in the figure legends and in the result section, one-way analysis of variance was used followed by post hoc testing (Bonferroni, Dunnett and Tukey) for multiple comparisons. Two-tailed unpaired Student's *t* test analysis was performed for comparisons between two groups using Prism (GraphPad, San Diego, CA). A value of $p \leq 0.05$ was considered statistically significant.

3. Results

3.1. KOR Activation upregulates DAT

3.1.1. SalA Increases DAT Function via KOR Activation—Addition of SalA to EM4 cells coexpressing KOR and DAT produced a concentration dependent increase in ASP^+ accumulation rate ($F_{(3, 211)} = 11.50$; $p \leq 0.0001$) (Fig. 1A). Increased accumulation occurred within 2 min after ASP^+ addition and persisted for at least 10 min. At 10 μM SalA, the magnitude of stimulation of ASP^+ accumulation rate varied between experiments with a minimum of ∼20% to a maximum of ∼60%. ASP^+ uptake as well as SalA-mediated

increase in the ASP^+ accumulation was also blocked by DAT inhibitor GBR 12909 ($F_{(4,521)}$ =213; $p < 0.0001$) (Fig. 1B). GBR 12909 insensitive ASP^+ accumulations found in cells coexpressing DAT and KOR was similar to ASP^+ accumulation in non-transfected cells (Fig. 1B). SalA was found to be a highly potent and selective KOR agonist. In order to validate whether SalA mediated stimulation of DAT activity was attributable to KOR, the effect of SalA was assessed in the presence of a selective KOR antagonist, nor-binaltorphimine (BNI). EM4 cells were preincubated for 10 min with BNI (1 μM) prior to the addition of vehicle or SalA (10 μM) followed by measuring ASP^+ accumulation and was compared with vehicle treatment (Fig. 1D). While SalA increased DAT activity in the absence of BNI, it did not alter DAT activity in the presence of BNI ($F_{(3,212)}$ =129; $p \leq 0.0001$). On the other hand, SalA increased ASP^+ uptake both in the presence and absence of D_2 receptor antagonist, L-741,626 (Fig. 1C). Furthermore, SalA treatment of EM4 cells expressing only the DAT did not produce any effect on DAT activity (Fig. 1C). These results indicate that SalA induced stimulation of DAT is KOR mediated.

3.1.2. Other KOR Agonists Increase DAT Function Via KOR Activation—Next we sought to examine whether SalA mediated DAT upregulation is unique to SalA or general consequence of KOR activation. We tested the effect of other known KOR agonists including U69,593 and U50,488 on DAT-mediated ASP^+ accumulation in EM4 cells coexpressing KOR and DAT. Similar to SalA, both U69,593 and U50,488 at 10 μM increased ASP^+ accumulation ($F_{(3, 3175)}$ =29.12; $p \leq 0.0001$) (Fig. 1B). However, preincubation of BNI (1 μM) for 10 min prior to the addition of vehicle or U69,593 or U50,488 completely blocked the stimulatory effect on DAT activity ($F_{(5,270)}$ =18.73; $p \leq 0.0001$) (Fig. 1B), suggesting the involvement of KOR. Kinetic analysis of ASP^+ uptake in EM4 cells coexpressing the DAT and KOR proteins showed that SalA (10 μM) treatment significantly increased the values of V_{max} (vehicle: 1.09 ± 0.07 AFUs; SalA: 1.49 ± 0.89 AFUs; t= 3.24, df=741; $p < 0.001$) and the values of K_m (vehicle: 2.74 ± 0.55 μM; SalA: 5.31 ± 0.85 μM; t= 2.15, df=741; $p < 0.03$). Thus, SalA increased the maximal velocity while decreasing the affinity.

3.1.3. Differential Influence of SalA on Serotonin and Norepinephrine Transporters—We next asked whether SalA regulates other amine transporters. Treatment with SalA (10 μM, 10 min) significantly reduced SERT-mediated ASP^+ accumulation in EM4 cells coexpressing KOR and human SERT (t=9.85, df=44 $p<0.0001$) (Fig 1C). BNI pretreatment blocked the decrease in SERT activity induced by SalA (t=8.31, df=26 $p<0.0001$) (Fig 1C). Kinetic analysis of ASP^+ uptake by SERT revealed a significant decrease in V_{max} value (vehicle: 1.93 ± 0.47 AFUs; SalA: 0.86 ± 0.21 AFUs; t=2.08, df=510 $p<0.04$) with no significant change in K_m value following SalA treatment (vehicle: 9.46 ± 4.01 μM; SalA: 2.88 ± 2.89 μM; t= 1.34, df=519; p =0.18). On the other hand, SalA (10 μM) and or BNI did not alter ASP^+ accumulation in EM4 cells co-expressing KOR and NET ($p > 0.1$) (Fig 1C). These results collectively indicate that SalA exhibits differential effect on DAT and SERT while it has no influence on NET.

3.1.4. SalA-KOR Mediated DAT Upregulation is Dependent on Gi/Go and ERK1/2 Activation—KOR is predominantly coupled to pertussis toxin (PTX) sensitive

Gi/Go types of G proteins and triggers diverse signaling systems including ERK1/2 (Bruchas and Chavkin, 2010). Therefore, we examined whether SalA-KOR-mediated stimulation of DAT activity requires Gi/Go and ERK1/2 activation. Pretreatment of EM4 cells coexpressing DAT and KOR with PTX (100 ng/ml for 16-24 hr) prevented SalA-mediated increase in ASP^+ uptake (Fig. 2A, $F_{(3,268)}$ =74.56, p = 0.0001). Next we examined whether SalA treatment activates ERK1/2 and p38 MAPK in EM4 cells co-expressing DAT and KOR by measuring ERK1/2 and p38 MAPK phosphorylation. Five min incubation of EM4 cells with SalA (10 μM) produced a significant (t-test; $p \leq 0.0001$; n=3) ∼2.5-fold increase in pERK1/2 levels with out any changes in total ERK1/2 confirming ERK1/2 activation by SalA (Fig. 2B). Similar to SalA, 5 min exposure of U69,593 (10 μM, ∼ 3 fold, t-test; $p \leq 0.005$; n=3) or U50,488 (10 μM, ∼ 3.5 fold t-test; $p \leq 0.008$; n=3) significantly increased pERK1/2 levels (Fig. 2B) with out altering total ERK1/2 expression. However, parallel analysis of the level of phospho-p38 MAPK and total p38 MAPK showed no significant changes ($F_{(5,30)} = 1.67$, p = 0.17) suggesting that KOR activation through SalA or U69,593 or U50,488 activates ERK1/2, but not p38 MAPK under the experimental conditions used. Incubation of cells with the ERK1/2 kinase inhibitor, PD98059 (10 μM), did not alter ASP^+ uptake but prevented SalA-evoked increases in ASP^+ accumulation (Fig. 2C; $F_{(3,278)} = 42.23$, p = 0.001). In contrast, pretreatment of cells with the p38 MAPK inhibitor, SB203580 (3 μM; 5 min), was ineffective in attenuating SalA-evoked increases in ASP^+ accumulation rate (% increase in slope: Veh/SalA = 28.29 ± 2.9%; SB203580/SalA= 36.42 ± 6.6%; t=1.4; df =156, $p > 0.15$ n=39). Parallel analysis showed that, PD98059 specifically reduced the SalA induced pERK1/2 level with no effect on phospho- p38 MAPK or total ERK1/2 and or total p38 MAPK. These results are consistent with our observations that SalA triggers ERK1/2 activation and subsequently upregulates DAT but not p38 MAPK.

3.2. SalA Upregulates DA Clearance in Rat Striatum via ERK1/2

The above results (Figs. 1 & 2) revealed that SalA triggers DAT activity through KOR-linked ERK1/2 activation in heterologous coexpressing cell model. Next we sought to examine whether SalA upregulates DAT function in native tissue. Given the fact that KOR is expressed in striatal dopamine axons and varicosities (Svingos et al., 2001), RDE voltammetry and radiolabelled DA uptake was performed in mince preparations of striatal tissue or synaptosomes respectively, to determine the effect of KOR activation on DAT function. Analogous to our results using heterologous expression systems, SalA as well as U50,488 significantly increased DAT mediated DA-transport in a GBR12909-sensitive manner (Fig. 3A; $F_{(2,30)} = 7.03$, p = 0.003) and was blocked by the presence of BNI ($F_{(4,37)}$ = 7.06, p = 0.0003) suggesting specific KOR-mediated effect on DAT. Furthermore, the ERK1/2 inhibitor PD98059 (10 μM) pretreatment (30 min) attenuated the SalA evoked DAT function Fig. 3B. PD98059 at 10 μM concentration did not affect dopamine clearance significantly ($F_{(1,16)} = 1.3$; p = 0.3), but it attenuated the SalA-evoked increase in DA clearance ($F_{(1,16)} = 5.1$; p = 0.04).

3.3. SalA Increases DAT Vmax

The kinetic parameters of the DAT (Michaelis–Menten constant, Km, and maximal velocity, Vmax) were determined in vehicle and SalA (10 μM; 5 min) treated striatal synaptosomes

(Fig. 4). DAT-specific DA transport was determined in the presence of the NET blocker nisoxetine (see details under methods and materials). SalA treatment increased the maximal velocity (Vmax) significantly from 27.8 ± 4.4 to 45.10 ± 1.0 pmol/mg protein per minute (t= 3.84, df=4; p <0.009) with no significant changes in the Km (vehicle: 29.77 ± 1.24 nM; SalA: 35.11 ± 2.23 nM; t= 2.09, df= 4; p=0.105)

3.4. SalA Upregulates DAT Cell Surface Expression

To determine whether up-regulation of DAT function is associated with increased DAT cell surface expression, surface biotinylation studies were conducted in EM4 cells coexpressing KOR and DAT (Fig. 5A). Consistent with the uptake data, SalA exposure of cells for 10 min significantly increased biotinylated DAT (% of vehicle, 214.3 ± 18.31 %, p = 0.0001). Treatment with SalA did not alter the total amount of DAT protein (Fig. 5A). Next, a rat striatal synaptosome preparation was used for biotinylation studies to examine whether SalA increases surface DAT in endogenously expressing preparations (Fig. 5B). Similar to the cell model, and consistent with the change in V_{max} of DA clearance, SalA exposure of striatal synaptosomes resulted in a significant increase in surface DAT (% of vehicle, 183.7 ± 13.2 %, p = 0.0001) without altering the total level of the DAT protein (Fig. 5B). Furthermore, pretreatment of cells or striatal synaptosomes with the ERK1/2 inhibitor PD98059 (10 μM, 30 min) blocked the SalA induced increase in surface DAT and synaptosomes (in % of vehicle; cells: Veh/SalA: 214.3 ± 18.31%, PD98050/SalA: 122.6 ± 3.0 %, p=0.0007; synaptosomes: Veh/SalA: 183.7 ± 13.2%, PD98050/SalA: 97.5 ± 14.4%, p=0.02). PD98059 at 10 μM concentration did not affect total and surface levels of DAT (Fig. 5A & B). We validated our surface biotinylation experiments for cellular integrity by determining the presence of intracellular calnexin in biotinylated fractions. Both in cells and synaptosomal experiments, less than 0.5% of total calnexin was present in biotinylated fractions suggesting that surface membranes were intact and intracellular proteins were not significantly biotinylated and contaminated/recovered with surface biotinylated proteins (data not shown).

3.5. DAT and KOR Interaction

3.5.1. DAT and KOR Exist in a Physical Complex—Our previous studies demonstrated that DAT and presynaptic D2s-Receptor form a stable complex (Bolan et al., 2007). Furthermore, Lee et al. established a direct interaction of the N-terminus of DAT with the third intracellular loop of the D2 receptor (Lee et al., 2007). Given the fact that both DAT and KOR are coexpressed in presynaptic DA-terminals (Svingos et al., 2001), and KOR activation upregulates DAT surface levels, we postulated that DAT and KOR might co-exist in a complex. To determine whether KOR and DAT formed interacting complexes we used three approaches to investigate the DAT-KOR association: co-immunoprecipitation, BRET and FRET in live cells to quantify the dynamics of DAT-KOR association. First, co-immunoprecipitation experiments were carried out in cells coexpressing myc-KOR and FLAG-DAT. Immunoprecipitation of myc-KOR with anti-myc antibody followed by immunoblotting with anti-DAT antibody revealed a ∼ 85 kDa band corresponding to mature, monomeric DAT in cells co-expressing both DAT and KOR proteins (Fig. 6A lane 2). No specific DAT band was observed when Protein A beads were used with non-transfected cellular extracts which indicates the specificity of the myc-

antibody to the immunoprecipitated myc-KOR protein (Fig. 6A lane 3). Furthermore, no specific DAT band was observed in the anti-myc-KOR immunocomplex isolated from the mixture of lysates that were prepared from cells expressing myc-KOR alone or FLAG-DAT alone (Fig. 6A lane 1). These results suggest that the formation of DAT-KOR complexes requires the expression of DAT and KOR in the same cell and rules out a simply an artefact due to solubilization and immunoprecipitation processes. Due to the presence of IgG in the eluate from the immunocomplex and as a result of cross immunoreactivity with secondary antibody, IgG bands were detected. In addition, to determine whether DAT/KOR complexes also exist in native tissues, we blotted DAT immunoprecipitates from rat striatal synaptosomes for KOR (Fig 6B). Immunoblotting of DAT immunoprecipitates (obtained using two different DAT antibodies) with a polyclonal KOR antibody revealed the presence of a ∼45 kDa band consistent with the expected size for KOR. In parallel experiments, the ∼45 kDa band is not immunoprecipitated from striatal extract when an irrelevant IgG (with Protein A sepharose) is utilized for immunoprecipitations (Fig 6B). Second, we used BRET (Angers et al., 2000) to determine whether DAT and KOR proteins are in close proximity (<100.Å) to form interacting complexes (Fig. 6C & D). Co-expression of Luc-KOR and DAT produced a positive energy transfer signal and an increased BRET ratio indicating that Luc-KOR and DAT-YFP are in close proximity (<100 Å). In accord with previous studies, an increased BRET ratio was observed in Luc-KOR and YFP-DOR expressing cells (Gomes et al., 2003). No energy transfer occurred in cells co-expressing Luc-KOR and YFP-CCR5 (Fig. 6C & D); thus, validating our BRET experiments. Third, to further evaluate whether DAT and KOR directly interact in living cells, we used FRET microscopy (Schmid and Sitte, 2003) using the three-filter method according to Xia and Lou (2001) (Xia and Liu, 2001). Quantitative visualization of protein oligomerization in intact cells was achieved by utilization of the IMAGE J imaging software (Feige et al., 2005) which allows to generate nFRET images. We co-expressed CFP-DAT and YFP-KOR (C-DAT and Y-KOR, respectively) and observed robust nFRET -signals (24.16 ± 1.7, n = 33; Fig. 7A & B): this confirms the formation of C-DAT and Y-KOR oligomers in living cells. To signify our FRET data, we also employed a membrane bound form of CFP that predominantly inserts into the plasma membrane but expectedly does not physically interact with Y-KOR; co-expression of a membrane attached CFP and Y-KOR yielded a nFRET value of 11.33 + 1.1 (n = 27; Fig. 7A & B), which was highly significant from the C-DAT/Y-KOR combination ($p < 0.001$). Apparently, this membrane attached CFP can serve as a weak acceptor for YFP fluorophores attached to proteins integral to membranes; indeed some spurious FRET signal was visible upon co-expression with Y-KOR (Fig. 7A & B). Therefore, we sought to determine if other membrane proteins interacted with Y-KOR similar to C-DAT. We examined two CFP-labelled, closely related NSS-family members, namely the human serotonin transporter (C-SERT) and the rat GABA transporter (C-GAT1; (Schmid et al., 2001)). However, although these two transport proteins nicely expressed at the cell surface (Fig. 7A) they only interacted spuriously with co-expressed Y-KOR at the extent of membrane bound CFP (Fig. 7A & B). Importantly, a quantification of fluorescent images included in this study showed no statistical significant difference in the expression levels of Y-KOR or ($F_{(3,110)} = 0.082$; $p = 0.97$) or CFP-tagged transporters (C-DAT or C-GAT1 or C-SERT) and membr.CFP ($F_{(3,110)} = 0.053$; $p = 0.98$) (Fig. 7C).

3.5.2. Salvinorin A Enhances the Interaction of DAT and KOR—Two significant results described so far led us to ask whether activation of KOR upon SalA binding could increase the DAT-KOR association to trigger appropriate signals to regulate DAT activity: (i) the effect of SalA on KOR-signaling that resulted in an increase in DAT activity and (ii) the existence of DAT and KOR as a complex. To determine whether SalA influences the existence of a DAT-KOR complex, the FRET analysis was conducted in HEK cells coexpressing C-DAT and Y-KOR (Fig. 7A & B). nFRET-values increased significantly after (1 min) the addition of 10 μM SalA and stayed constant up to 5 min (Fig. 8A & B) ($p < 0.01$, ANOVA with Tukey's multiple comparison test).

4. Discussion

Dopamine neurotransmission is regulated by modulation of dopamine release and DAT-mediated uptake. SalA and synthetic KOR agonists decrease dopamine release in striatal sub-regions. This action is thought to underlie the dysphoric and pro-depressant like effects of these drugs. In addition, KOR agonists attenuate cocaine self-administration in rats and reinstatement of cocaine seeking produced by experimenter-administered cocaine (Morani et al., 2009; Schenk et al., 1999). They produce pro-depressant like effects in rodent models (Todtenkopf et al., 2004). These effects have been linked to agonist-induced decreases in dopamine release in brain regions subserving mood and motivation and subsequent changes in dopamine transmission. Thus, the KOR system exerts an inhibitory control on DA release in ventral striatum (Chefer et al., 2005; Heijna et al., 1990; Spanagel et al., 1992) and mPFC cortex (Tejeda et al., 2013). Recent studies have demonstrated that, in mice, specific deletion of KOR in dopaminergic neurons leads to anxiolytic-like effect on behaviour, enhanced cocaine induced plasticity and disrupts development of KOR-mediated conditional place aversion (Chefer et al., 2013; Tejeda et al., 2013; Van't Veer et al., 2013). More significantly while KOR agonist U69,593 decreased DA overflow in nucleus accumbens and prefrontal cortex in wild type mice, KOR agonist U69,593 had no effect in mice expressing DA neurons with out KOR (Chefer et al., 2013; Tejeda et al., 2013). Although, these findings signify an important role for the KOR in DA neurons in the regulation of dopaminergic neurotransmission and KOR-mediated behaviours, DAT functional expression and regulation need to be investigated. The present studies, prompted by the demonstration that KOR and DAT are apposed in dopamine axonal varicosities (Svingos et al., 2001), demonstrate that SalA rapidly increases DAT function both in heterologous cells and striatal tissue through activating KOR and ERK1/2. Furthermore, we provide evidence for the presence of physical association of DAT with KOR and that association DAT and KOR enhanced upon SalA exposure.

4.1. SalA and other KOR agonists alter biogenic amine transporters function differentially via a BNI–reversible mechanism

Quantification of ASP^+ accumulation in cells transfected with KOR and DAT revealed a rapid increase in DAT function following SalA exposure. Pretreatment with the selective KOR antagonist, BNI, prevented the effect of SalA indicating that upregulation of DAT function is KOR mediated. Other KOR agonists also upregulated DAT function that is sensitive to BNI and thus, general activation of KOR appears to support DAT regulation. It

has been shown that SalA exhibits stimulatory effect on dopamine D2 receptors (Beerepoot et al., 2008; Seeman et al., 2009). Since both heterologously expressed D_2R and endogenously expressed D_2R regulate DAT activity (Bolan et al., 2007; Lee et al., 2007; Mayfield and Zahniser, 2001; Zapata et al., 2007); (Bowton et al.), it raises the question whether D_2R activation is involved in SalA mediated DAT upregulation. However, D_2R antagonist L-741,626 (Bowery et al., 1996) did not affect SalA induced increase in DAT activity. In addition, SalA induced DAT activation is observed only in cells coexpressing both DAT and KOR, but not in cells expressing DAT alone. These results confirm the involvement of KOR, but not D_2R in SalA induced stimulation of DAT activity. Interestingly, SalA exhibits differential influence on amine transporters in that it increases DAT function and decreases SERT function while having no effect on NET function. A recent study demonstrated that U50,488 induced upregulation of SERT activity and surface expression require p38α MAPK in serotonergic neurons *in vivo* and implicated to stress-linked neuronal events (Bruchas et al., 2011). Thus this differential regulation of aminergic neurotransmission by SalA may have consequences on KOR-linked behavioural out put. It is also possible that differential regulation of aminergic neurotransmission may vary among KOR agonists as well as to different environment.

4.2. SalA upregulates DAT function in PTX sensitive and ERK1/2-dependent mechanism

The finding that PTX prevented SalA-evoked increases in ASP^+ accumulation indicates that upregulation is Gi/Go-dependent. KOR activation induces ERK1/2 phosphorylation (Belcheva et al., 2005; Bohn et al., 2000; Bruchas et al., 2008; Potter et al., 2011) for reviews, see (Bruchas and Chavkin, 2010) and ERK1/2 modulates DAT function and cell surface expression (Moron et al., 2003). Immunoblotting confirmed that SalA induces pERK in EM4 cells coexpressing KOR and DAT. Furthermore, inhibition of this kinase prevented SalA evoked upregulation of DAT function. The concentration of PD98059 used was lower than that which inhibits DAT function (Moron et al., 2003). Therefore, the attenuated response to SalA cannot be attributed to effects of the inhibitor alone. These data provide the first demonstration that KOR regulates DAT via an ERK1/2-dependent mechanism. KOR is also coupled to p38 MAPK activation demonstrated *in vivo* (Bruchas et al., 2011; Lemos et al., 2012). However treatment of SalA, U69,593 or U50,488 for 5 min did not increase phospho-p38 MAPK immunoreactivity. Consistently, inhibition of p38 MAPK failed to modify the effect of SalA indicating a specific role for the ERK1/2 cascade in mediating the functional modulation of DAT by this KOR agonist. In addition, Moron et al reported that p38 MAPK inhibitor, SB 203580 failed to affect DAT activity in rat striatal synaptosomes (Moron et al., 2003). It has been known that the KOR-mediated intracellular signaling cascades vary depending on the cell model used as well as the ligand, dose and duration of treatment, reviewed in (Bruchas and Chavkin, 2010).

4. 3. KOR activation by SalA and U50,488 increases DA clearance in striatum and SalA-mediated DAT upregulation is ERK1/2 dependent

Studies using rat striatum revealed a BNI-sensitive rapid increase in dopamine clearance following acute SalA or U50,488 exposure. Analogous to cells, ERK1/2 inhibition attenuated the increase in striatal DAT function produced by SalA. These findings are noteworthy. They demonstrate that SalA increases DAT function in native tissue by an

ERK1/2-dependent mechanism. Furthermore, they indicate that the functional interaction of KOR and DAT observed in heterologous systems is not due to high levels or artificial co-expression of these proteins. Moreover, ERK1/2 activation has been documented in the nucleus accumbens of acute and repeated SalA administered rats (Potter et al., 2011). Kinetic analysis revealed a marked increase in the V_{max} of DA or ASP^+ transport in EM4 cells coexpressing DAT/KOR and in striatal synaptosomes respectively. However, while SalA did not alter K_m for DA in striatal synaptosomes, SalA increased K_m for ASP^+ uptake in EM4 cells coexpressing DAT/KOR. Such differences could reflect the specific nature of regulatory mechanisms in different environments (native *versus* heterologous), or DAT and KOR coexpression ratio or other unknown processes that could affect DAT kinetics differently. It may simply reflect sampling bias inherent in the single-cell assay conditions of ASP^+ uptake (fluorescence microscopy *versus* radiometric techniques) or use of native DAT substrates DA *versus* ASP^+ to assay DAT activity. Therefore, it is possible that KOR mediated DAT regulation may vary based on the environment as well as brain regions. Acute systemic administration of synthetic KOR agonists increases dopamine transport *ex-vivo* in ventral but not dorsal striatum (Thompson et al., 2000). Moreover, *in-vivo* quantitative microdialysis revealed no effect of systemic administration or local perfusion of SalA on dopamine uptake in dorsal striatum (Gehrke et al., 2008). However, data regarding the effects of SalA on basal dopamine clearance in ventral striatum are lacking. In the present study, RDE voltammetry was performed in mince preparations of the dorsal and ventral striatum and therefore it is difficult to conclude whether SalA mediated increase in DAT-activity occurs in both regions or region specific. In this context, we recently reported that KOR agonist U69,593 does not modify DAT- or NET-mediated DA uptake in mPFC synaptosomes and conditional deletion of KORs on DA neurons does not change DA uptake in mPFC assessed with no-net-flux microdialysis (Tejeda et al., 2013). Alternatively, the half-life of SalA is short, ranging from 8-36 min (Hooker et al., 2008; Schmidt et al., 2005). Therefore, the longer sampling duration required for microdialysis (e.g. >30 min) relative to that of voltammetry (sec) may underlie the observed lack of effect in dorsal striatum.

4.4. KOR activation enhances DAT cell surface expression

Changes in V_{max} are often due to alterations in protein trafficking. Constitutive DAT trafficking between the membrane and intracellular compartments has been reported (Loder and Melikian, 2003). Changes in trafficking enable rapid regulation of dopamine transmission. Surface biotinylation studies revealed the enhanced surface DAT availability following SalA exposure in both cells and native tissue suggesting that SalA increase DAT function, in part, by promoting redistribution of DAT to the cell surface. Consistent with the blockade effect of ERK1/2 inhibition on SalA induced upregulation of DAT activity, inhibition of ERK1/2 prevented SalA triggered increase in surface DAT. However, level of SalA induced DAT surface enhancement is higher than uptake suggesting the involvement of multiple stages of transporter trafficking and catalytic activation and or due to different assays employed (uptake versus biotinylationimmunoblot). It is noteworthy that regulation of PKG and p38 MAPK-dependent SERT regulation has been associated with enhancement of surface SERT followed by catalytic activation (Zhu et al., 2004). We have demonstrated that activation of D3-dopamine receptor regulates DAT trafficking at the level of DAT endocytosis - exocytosis – recycling in a biphasic manner to regulate surface DAT

expression and function (Zapata et al., 2007). Further research is needed to fully identify additional cellular mechanisms involved in the regulation of SalA-KOR mediated DAT upregulation.

4.5. DAT and KOR exists in a physical complex

Co-immunoprecipitation studies from transfected cells coexpressing KOR and DAT and striatal tissue suggest that KOR and DAT exist in a physical complex. Furthermore, BRET experiments revealed energy transfer between Luc-KOR and YFP-DAT suggesting that they are in close proximity. Importantly, energy transfer can arise from random interactions within the membrane when high expression levels and single acceptor/donor ratios are employed (James et al., 2006). Furthermore, FRET studies confirmed the presence of a physical complex of DAT with KOR in living cells. Taken together, these results demonstrate that KOR and DAT are in sufficient proximity to interact, although an indirect interaction cannot be excluded. Interestingly, SalA treatment enhanced DAT-KOR assembly suggesting that activation of KOR promotes and/or regulate DAT-KOR assembling. Recently it has been demonstrated that A_3 adenosine receptor activation augments SERT-A_3 adenosine receptor complex formation (Zhu et al., 2011). Activation of NK1R triggers NET redistribution through raft-mediated translocation of NET-NK1R complexes and facilitates recruitment of signaling molecules (Arapulisamy et al., 2013). It is also possible that DAT activation/inhibition by DAT substrates and inhibitors respectively may regulate KOR-mediated DAT regulation and physical association of DAT and KOR.

4.6. Concluding remarks

Phosphorylation of monoamine transporters is one cellular mechanism by which protein kinases regulate amine uptake. DAT contains putative consensus sites for several protein kinases including potential phosphorylation sites for ERK (Ser-13, Thr-53; Thr-595) (Gorentla et al., 2009). Mutation of Thr-53 eliminates ERK triggered DAT phosphorylation providing direct evidence that Thr-53 is a phosphorylation site for ERK (Gorentla et al., 2009) and also has functional significance (Foster et al., 2012). These findings raise the possibility that ERK activation by SalA may promote DAT phosphorylation and this action may contribute to SalA-evoked DAT upregulation. Studies addressing this issue are currently in progress. Taken together, the results of the present study, demonstrating that SalA increases DAT function suggests that it may affect behaviour and dopamine neurotransmission by two distinct mechanisms, inhibition of release (Ebner et al., 2010) and ERK dependent upregulation of dopamine transport. Furthermore, the demonstration that KOR and DAT are in close proximity in both cells and native tissue (Svingos et al., 2001) provides a cellular basis by which SalA and synthetic KOR agonists (Thompson et al., 2000) regulate basal DAT function.

Acknowledgments

This work was supported by the National Institutes of Health and National Institute on Drug Abuse Intramural Research Program (T.S.S), NIH grants, MH083928, MH091633 (S.R), DA018151 (T.E.P), DA019521, DA08863, GM071558 (L.A.D.), The Health Research Council of New Zealand (B.K) and Austrian Science Fund/FWF, P23658 (H.H.S). CCRP-YFP was kindly provided by Dr Michel Bouvier (University of Montreal). DAT constructs were provided by Dr. Jonathan Javitch.

References

Adkins EM, Samuvel DJ, Fog JU, Eriksen J, Jayanthi LD, Vaegter CB, Ramamoorthy S, Gether U. Membrane mobility and microdomain association of the dopamine transporter studied with fluorescence correlation spectroscopy and fluorescence recovery after photobleaching. Biochemistry. 2007; 46:10484–10497. [PubMed: 17711354]

Alessi DR, Cuenda A, Cohen P, Dudley DT, Saltiel AR. PD 098059 is a specific inhibitor of the activation of mitogen-activated protein kinase kinase in vitro and in vivo. J Biol Chem. 1995; 270:27489–27494. [PubMed: 7499206]

Amara S, Kuhar M. Neurotransmitter Transporters - Recent Progress. Annual Review of Neuroscience. 1993; 16:73–93.

Angers S, Salahpour A, Joly E, Hilairet S, Chelsky D, Dennis M, Bouvier M. Detection of beta 2-adrenergic receptor dimerization in living cells using bioluminescence resonance energy transfer (BRET). Proc Natl Acad Sci U S A. 2000; 97:3684–3689. [PubMed: 10725388]

Arapulisamy O, Mannangatti P, Jayanthi LD. Regulated Norepinephrine Transporter Interaction with the Neurokinin-1 Receptor Establishes Transporter Subcellular Localization. J Biol Chem. 2013; 288:28599–28610. [PubMed: 23979140]

Bartholomaus I, Milan-Lobo L, Nicke A, Dutertre S, Hastrup H, Jha A, Gether U, Sitte HH, Betz H, Eulenburg V. Glycine transporter dimers: evidence for occurrence in the plasma membrane. J Biol Chem. 2008; 283:10978–10991. [PubMed: 18252709]

Beerepoot P, Lam V, Luu A, Tsoi B, Siebert D, Szechtman H. Effects of salvinorin A on locomotor sensitization to D2/D3 dopamine agonist quinpirole. Neurosci Lett. 2008

Belcheva MM, Clark AL, Haas PD, Serna JS, Hahn JW, Kiss A, Coscia CJ. Mu and kappa opioid receptors activate ERK/MAPK via different protein kinase C isoforms and secondary messengers in astrocytes. J Biol Chem. 2005; 280:27662–27669. [PubMed: 15944153]

Bohn LM, Belcheva MM, Coscia CJ. Mitogenic signaling via endogenous kappa-opioid receptors in C6 glioma cells: evidence for the involvement of protein kinase C and the mitogen-activated protein kinase signaling cascade. J Neurochem. 2000; 74:564–573. [PubMed: 10646507]

Bolan EA, Kivell B, Jaligam V, Oz M, Jayanthi LD, Han Y, Sen N, Urizar E, Gomes I, Devi LA, Ramamoorthy S, Javitch JA, Zapata A, Shippenberg TS. D2 receptors regulate dopamine transporter function via an extracellular signal-regulated kinases 1 and 2-dependent and phosphoinositide 3 kinase-independent mechanism. Mol Pharmacol. 2007; 71:1222–1232. [PubMed: 17267664]

Bowery BJ, Razzaque Z, Emms F, Patel S, Freedman S, Bristow L, Kulagowski J, Seabrook GR. Antagonism of the effects of (+)-PD 128907 on midbrain dopamine neurones in rat brain slices by a selective D2 receptor antagonist L-741,626. Br J Pharmacol. 1996; 119:1491–1497. [PubMed: 8968560]

Bowton E, Saunders C, Erreger K, Sakrikar D, Matthies HJ, Sen N, Jessen T, Colbran RJ, Caron MG, Javitch JA, Blakely RD, Galli A. Dysregulation of dopamine transporters via dopamine D2 autoreceptors triggers anomalous dopamine efflux associated with attention-deficit hyperactivity disorder. J Neurosci. 30:6048–6057. [PubMed: 20427663]

Bruchas MR, Chavkin C. Kinase cascades and ligand-directed signaling at the kappa opioid receptor. Psychopharmacology (Berl). 2010; 210:137–147. [PubMed: 20401607]

Bruchas MR, Schindler AG, Shankar H, Messinger DI, Miyatake M, Land BB, Lemos JC, Hagan CE, Neumaier JF, Quintana A, Palmiter RD, Chavkin C. Selective p38alpha MAPK deletion in serotonergic neurons produces stress resilience in models of depression and addiction. Neuron. 2011; 71:498–511. [PubMed: 21835346]

Bruchas MR, Xu M, Chavkin C. Repeated swim stress induces kappa opioid-mediated activation of extracellular signal-regulated kinase 1/2. Neuroreport. 2008; 19:1417–1422. [PubMed: 18766023]

Butelman ER, Mandau M, Tidgewell K, Prisinzano TE, Yuferov V, Kreek MJ. Effects of salvinorin A, a kappa-opioid hallucinogen, on a neuroendocrine biomarker assay in nonhuman primates with high kappa-receptor homology to humans. J Pharmacol Exp Ther. 2007; 320:300–306. [PubMed: 17060493]

Carvelli L, Moron JA, Kahlig KM, Ferrer JV, Sen N, Lechleiter JD, Leeb-Lundberg LM, Merrill G, Lafer EM, Ballou LM, Shippenberg TS, Javitch JA, Lin RZ, Galli A. PI 3-kinase regulation of dopamine uptake. J Neurochem. 2002; 81:859–869. [PubMed: 12065645]

Chakrabarti S, Liu NJ, Gintzler AR. Formation of mu-/kappa-opioid receptor heterodimer is sex-dependent and mediates female-specific opioid analgesia. Proc Natl Acad Sci U S A. 2010; 107:20115–20119. [PubMed: 21041644]

Chefer VI, Backman CM, Gigante ED, Shippenberg TS. Kappa Opioid Receptors on Dopaminergic Neurons Are Necessary for Kappa-Mediated Place Aversion. Neuropsychopharmacology. 2013

Chefer VI, Czyzyk T, Bolan EA, Moron J, Pintar JE, Shippenberg TS. Endogenous kappa-opioid receptor systems regulate mesoaccumbal dopamine dynamics and vulnerability to cocaine. J Neurosci. 2005; 25:5029–5037. [PubMed: 15901784]

Dalman FC, O'Malley KL. kappa-Opioid tolerance and dependence in cultures of dopaminergic midbrain neurons. J Neurosci. 1999; 19:5750–5757. [PubMed: 10407016]

Doolen S, Zahniser NR. Protein tyrosine kinase inhibitors alter human dopamine transporter activity in Xenopus oocytes. J Pharmacol Exp Ther. 2001; 296:931–938. [PubMed: 11181926]

Ebner SR, Roitman MF, Potter DN, Rachlin AB, Chartoff EH. Depressive-like effects of the kappa opioid receptor agonist salvinorin A are associated with decreased phasic dopamine release in the nucleus accumbens. Psychopharmacology (Berl). 2010; 210:241–252. [PubMed: 20372879]

Eriksen J, Jorgensen TN, Gether U. Regulation of dopamine transporter function by protein-protein interactions: new discoveries and methodological challenges. J Neurochem. 2010; 113:27–41. [PubMed: 20085610]

Feige JN, Sage D, Wahli W, Desvergne B, Gelman L. PixFRET, an ImageJ plug-in for FRET calculation that can accommodate variations in spectral bleed-throughs. Microsc Res Tech. 2005; 68:51–58. [PubMed: 16208719]

Fog JU, Khoshbouei H, Holy M, Owens WA, Vaegter CB, Sen N, Nikandrova Y, Bowton E, McMahon DG, Colbran RJ, Daws LC, Sitte HH, Javitch JA, Galli A, Gether U. Calmodulin kinase II interacts with the dopamine transporter C terminus to regulate amphetamine-induced reverse transport. Neuron. 2006; 51:417–429. [PubMed: 16908408]

Foster JD, Vaughan RA. Palmitoylation Controls Dopamine Transporter Kinetics, Degradation, and Protein Kinase C-dependent Regulation. J Biol Chem. 2011; 286:5175–5186. [PubMed: 21118819]

Foster JD, Yang JW, Moritz AE, Challasivakanaka S, Smith MA, Holy M, Wilebski K, Sitte HH, Vaughan RA. Dopamine transporter phosphorylation site threonine 53 regulates substrate reuptake and amphetamine-stimulated efflux. J Biol Chem. 2012; 287:29702–29712. [PubMed: 22722938]

Garcia BG, Wei Y, Moron JA, Lin RZ, Javitch JA, Galli A. Akt is essential for insulin modulation of amphetamine-induced human dopamine transporter cell-surface redistribution. Mol Pharmacol. 2005; 68:102–109. [PubMed: 15795321]

Gehrke BJ, Chefer VI, Shippenberg TS. Effects of acute and repeated administration of salvinorin A on dopamine function in the rat dorsal striatum. Psychopharmacology (Berl). 2008; 197:509–517. [PubMed: 18246329]

Gomes I, Filipovska J, Devi LA. Opioid receptor oligomerization. Detection and functional characterization of interacting receptors. Methods Mol Med. 2003; 84:157–183. [PubMed: 12703323]

Gorentla BK, Moritz AE, Foster JD, Vaughan RA. Proline-directed phosphorylation of the dopamine transporter N-terminal domain. Biochemistry. 2009; 48:1067–1076. [PubMed: 19146407]

Granas C, Ferrer J, Loland CJ, Javitch JA, Gether U. N-terminal truncation of the dopamine transporter abolishes phorbol ester- and substance P receptor-stimulated phosphorylation without impairing transporter internalization. J Biol Chem. 2003; 278:4990–5000. [PubMed: 12464618]

Griffin OH, Miller BL, Khey DN. Legally high? Legal considerations of Salvia divinorum. J Psychoactive Drugs. 2008; 40:183–191. [PubMed: 18720668]

Grilli M, Neri E, Zappettini S, Massa F, Bisio A, Romussi G, Marchi M, Pittaluga A. Salvinorin A exerts opposite presynaptic controls on neurotransmitter exocytosis from mouse brain nerve terminals. Neuropharmacology. 2009; 57:523–530. [PubMed: 19628000]

Heijna MH, Padt M, Hogenboom F, Portoghese PS, Mulder AH, Schoffelmeer AN. Opioid receptor-mediated inhibition of dopamine and acetylcholine release from slices of rat nucleus accumbens, olfactory tubercle and frontal cortex. Eur J Pharmacol. 1990; 181:267–278. [PubMed: 2166675]

Hooker JM, Xu Y, Schiffer W, Shea C, Carter P, Fowler JS. Pharmacokinetics of the potent hallucinogen, salvinorin A in primates parallels the rapid onset and short duration of effects in humans. Neuroimage. 2008; 41:1044–1050. [PubMed: 18434204]

Hoover BR, Everett CV, Sorkin A, Zahniser NR. Rapid regulation of dopamine transporters by tyrosine kinases in rat neuronal preparations. J Neurochem. 2007; 101:1258–1271. [PubMed: 17419806]

James JR, Oliveira MI, Carmo AM, Iaboni A, Davis SJ. A rigorous experimental framework for detecting protein oligomerization using bioluminescence resonance energy transfer. Nat Methods. 2006; 3:1001–1006. [PubMed: 17086179]

Jordan BA, Devi LA. G-protein-coupled receptor heterodimerization modulates receptor function. Nature. 1999; 399:697–700. [PubMed: 10385123]

Just H, Sitte HH, Schmid JA, Freissmuth M, Kudlacek O. Identification of an additional interaction domain in transmembrane domains 11 and 12 that supports oligomer formation in the human serotonin transporter. J Biol Chem. 2004; 279:6650–6657. [PubMed: 14660642]

Khoshbouei H, Sen N, Guptaroy B, Johnson L, Lund D, Gnegy ME, Galli A, Javitch JA. N-terminal phosphorylation of the dopamine transporter is required for amphetamine-induced efflux. PLoS Biol. 2004; 2:0387–0393.

Lee FJ, Pei L, Moszczynska A, Vukusic B, Fletcher PJ, Liu F. Dopamine transporter cell surface localization facilitated by a direct interaction with the dopamine D2 receptor. Embo J. 2007; 26:2127–2136. [PubMed: 17380124]

Lemos JC, Roth CA, Messinger DI, Gill HK, Phillips PE, Chavkin C. Repeated stress dysregulates kappa-opioid receptor signaling in the dorsal raphe through a p38alpha MAPK-dependent mechanism. J Neurosci. 2012; 32:12325–12336. [PubMed: 22956823]

Li LB, Chen N, Ramamoorthy S, Chi L, Cui XN, Wang LC, Reith ME. The role of N-glycosylation in function and surface trafficking of the human dopamine transporter. J Biol Chem. 2004; 279:21012–21020. [PubMed: 15024013]

Loder MK, Melikian HE. The dopamine transporter constitutively internalizes and recycles in a protein kinase C-regulated manner in stably transfected PC12 cell lines. J Biol Chem. 2003; 278:22168–22174. [PubMed: 12682063]

Mayfield RD, Zahniser NR. Dopamine D2 receptor regulation of the dopamine transporter expressed in Xenopus laevis oocytes is voltage-independent. Mol Pharmacol. 2001; 59:113–121. [PubMed: 11125031]

Melikian HE. Neurotransmitter transporter trafficking: endocytosis, recycling, and regulation. Pharmacol Ther. 2004; 104:17–27. [PubMed: 15500906]

Miranda M, Wu CC, Sorkina T, Korstjens DR, Sorkin A. Enhanced ubiquitylation and accelerated degradation of the dopamine transporter mediated by protein kinase C. J Biol Chem. 2005; 280:35617–35624. [PubMed: 16109712]

Mizrahi R, Rusjan P, Agid O, Graff A, Mamo DC, Zipursky RB, Kapur S. Adverse subjective experience with antipsychotics and its relationship to striatal and extrastriatal D2 receptors: a PET study in schizophrenia. Am J Psychiatry. 2007; 164:630–637. [PubMed: 17403977]

Morani AS, Kivell B, Prisinzano TE, Schenk S. Effect of kappa-opioid receptor agonists U69593, U50488H, spiradoline and salvinorin A on cocaine-induced drug-seeking in rats. Pharmacol Biochem Behav. 2009; 94:244–249. [PubMed: 19747933]

Moron JA, Zakharova I, Ferrer JV, Merrill GA, Hope B, Lafer EM, Lin ZC, Wang JB, Javitch JA, Galli A, Shippenberg TS. Mitogen-activated protein kinase regulates dopamine transporter surface expression and dopamine transport capacity. J Neurosci. 2003; 23:8480–8488. [PubMed: 13679416]

Page G, Peeters M, Najimi M, Maloteaux JM, Hermans E. Modulation of the neuronal dopamine transporter activity by the metabotropic glutamate receptor mGluR5 in rat striatal synaptosomes through phosphorylation mediated processes. J Neurochem. 2001; 76:1282–1290. [PubMed: 11238713]

Potter DN, Damez-Werno D, Carlezon WA Jr, Cohen BM, Chartoff EH. Repeated exposure to the kappa-opioid receptor agonist salvinorin A modulates extracellular signal-regulated kinase and reward sensitivity. Biol Psychiatry. 2011; 70:744–753. [PubMed: 21757186]

Pramod AB, Foster J, Carvelli L, Henry LK. SLC6 transporters: structure, function, regulation, disease association and therapeutics. Mol Aspects Med. 2013; 34:197–219. [PubMed: 23506866]

Price DA, Sorkin A, Zahniser NR. Cyclin-dependent kinase 5 inhibitors: inhibition of dopamine transporter activity. Mol Pharmacol. 2009; 76:812–823. [PubMed: 19628755]

Ramamoorthy S, Shippenberg TS, Jayanthi LD. Regulation of monoamine transporters: Role of transporter phosphorylation. Pharmacol Ther. 2011; 129:220–238. [PubMed: 20951731]

Samuvel DJ, Jayanthi LD, Manohar S, Kaliyaperumal K, See RE, Ramamoorthy S. Dysregulation of dopamine transporter trafficking and function after abstinence from cocaine self-administration in rats: evidence for differential regulation in caudate putamen and nucleus accumbens. J Pharmacol Exp Ther. 2008; 325:293–301. [PubMed: 18198344]

Schenk S, Partridge B, Shippenberg TS. U69593, a kappa-opioid agonist, decreases cocaine self-administration and decreases cocaine-produced drug-seeking. Psychopharmacology (Berl). 1999; 144:339–346. [PubMed: 10435406]

Schmid JA, Scholze P, Kudlacek O, Freissmuth M, Singer EA, Sitte HH. Oligomerization of the human serotonin transporter and of the rat GABA transporter 1 visualized by fluorescence resonance energy transfer microscopy in living cells. J Biol Chem. 2001; 276:3805–3810. [PubMed: 11071889]

Schmid JA, Sitte HH. Fluorescence resonance energy transfer in the study of cancer pathways. Curr Opin Oncol. 2003; 15:55–64. [PubMed: 12490762]

Schmidt MD, Schmidt MS, Butelman ER, Harding WW, Tidgewell K, Murry DJ, Kreek MJ, Prisinzano TE. Pharmacokinetics of the plant-derived kappa-opioid hallucinogen salvinorin A in nonhuman primates. Synapse. 2005; 58:208–210. [PubMed: 16138318]

Schwartz JW, Blakely RD, DeFelice LJ. Binding and transport in norepinephrine transporters. Real-time, spatially resolved analysis in single cells using a fluorescent substrate. J Biol Chem. 2003; 278:9768–9777. [PubMed: 12499385]

Seeman P, Guan HC, Hirbec H. Dopamine D2High receptors stimulated by phencyclidines, lysergic acid diethylamide, salvinorin A, and modafinil. Synapse. 2009; 63:698–704. [PubMed: 19391150]

Shippenberg TS, Zapata A, Chefer VI. Dynorphin and the pathophysiology of drug addiction. Pharmacol Ther. 2007; 116:306–321. [PubMed: 17868902]

Spanagel R, Herz A, Shippenberg TS. The effects of opioid peptides on dopamine release in the nucleus accumbens: an in vivo microdialysis study. J Neurochem. 1990; 55:1734–1740. [PubMed: 1976759]

Spanagel R, Herz A, Shippenberg TS. Opposing tonically active endogenous opioid systems modulate the mesolimbic dopaminergic pathway. Proc Natl Acad Sci U S A. 1992; 89:2046–2050. [PubMed: 1347943]

Sucic S, Dallinger S, Zdrazil B, Weissensteiner R, Jorgensen TN, Holy M, Kudlacek O, Seidel S, Cha JH, Gether U, Newman AH, Ecker GF, Freissmuth M, Sitte HH. The N terminus of monoamine transporters is a lever required for the action of amphetamines. J Biol Chem. 2010; 285:10924–10938. [PubMed: 20118234]

Svingos AL, Chavkin C, Colago EE, Pickel VM. Major coexpression of kappa-opioid receptors and the dopamine transporter in nucleus accumbens axonal profiles. Synapse. 2001; 42:185–192. [PubMed: 11746715]

Tejeda HA, Counotte DS, Oh E, Ramamoorthy S, Schultz-Kuszak KN, Backman CM, Chefer V, O'Donnell P, Shippenberg TS. Prefrontal cortical kappa-opioid receptor modulation of local neurotransmission and conditioned place aversion. Neuropsychopharmacology. 2013; 38:1770–1779. [PubMed: 23542927]

Thompson AC, Zapata A, Justice JB Jr, Vaughan RA, Sharpe LG, Shippenberg TS. Kappa-opioid receptor activation modifies dopamine uptake in the nucleus accumbens and opposes the effects of cocaine. J Neurosci. 2000; 20:9333–9340. [PubMed: 11125013]

Tidgewell K, Harding WW, Schmidt M, Holden KG, Murry DJ, Prisinzano TE. A facile method for the preparation of deuterium labeled salvinorin A: synthesis of [2,2,2-2H3]-salvinorin A. Bioorg Med Chem Lett. 2004; 14:5099–5102. [PubMed: 15380207]

Todtenkopf MS, Marcus JF, Portoghese PS, Carlezon WA Jr. Effects of kappa-opioid receptor ligands on intracranial self-stimulation in rats. Psychopharmacology (Berl). 2004; 172:463–470. [PubMed: 14727002]

Van't Veer A, Bechtholt AJ, Onvani S, Potter D, Wang Y, Liu-Chen LY, Schutz G, Chartoff EH, Rudolph U, Cohen BM, Carlezon WA Jr. Ablation of kappa-opioid receptors from brain dopamine neurons has anxiolytic-like effects and enhances cocaine-induced plasticity. Neuropsychopharmacology. 2013; 38:1585–1597. [PubMed: 23446450]

Vaughan RA, Foster JD. Mechanisms of dopamine transporter regulation in normal and disease states. Trends Pharmacol Sci. 2013; 34:489–496. [PubMed: 23968642]

Vortherms TA, Roth BL. Salvinorin A: from natural product to human therapeutics. Mol Interv. 2006; 6:257–265. [PubMed: 17035666]

Xia Z, Liu Y. Reliable and global measurement of fluorescence resonance energy transfer using fluorescence microscopes. Biophys J. 2001; 81:2395–2402. [PubMed: 11566809]

Zapata A, Kivell B, Han Y, Javitch JA, Bolan EA, Kuraguntla D, Jaligam V, Oz M, Jayanthi LD, Samuvel DJ, Ramamoorthy S, Shippenberg TS. Regulation of dopamine transporter function and cell surface expression by D3 dopamine receptors. J Biol Chem. 2007; 282:35842–35854. [PubMed: 17923483]

Zhang L, Coffey LL, Reith MEA. Regulation of the functional activity of the human dopamine transporter by protein kinase C. Biochem Pharmacol. 1997; 53:677–688. [PubMed: 9113087]

Zhu CB, Hewlett WA, Feoktistov I, Biaggioni I, Blakely RD. Adenosine receptor, protein kinase G, and p38 mitogen-activated protein kinase-dependent up-regulation of serotonin transporters involves both transporter trafficking and activation. Mol Pharmacol. 2004; 65:1462–1474. [PubMed: 15155839]

Zhu CB, Lindler KM, Campbell NG, Sutcliffe JS, Hewlett WA, Blakely RD. Colocalization and regulated physical association of presynaptic serotonin transporters with A(3) adenosine receptors. Mol Pharmacol. 2011; 80:458–465. [PubMed: 21705486]

Abbreviations

ASP$^+$	trans 4-(4-(dimethylamino)-styryl)-N-methylpyridinium)
BNI	nor-binaltorphimine
BRET	Biolumiescence Resonance Energy Transfer
DAT	Dopamine transporter
ERK1/2	Extracellular signal-regulated kinases ½
FRET	Fluorescence Resonance Energy Transfer FRET
GPCR	G-protein coupled receptor
KOR	*kappa* Opioid receptor
SalA	Salvinorin A

Highlights

- Salvinorin A produces psychotomimesis, dysphoria and prodepressant like effects.
- Major determinant of aminergic signalling is the activity of amine transporters.
- We studied the effect of Salvinorin A on amine transporter function.
- Salvinorin A upregulates dopamine uptake and surface transporter via KOR-ERK1/2.
- κ-opioid receptor and dopamine transporter exist in a physical complex.

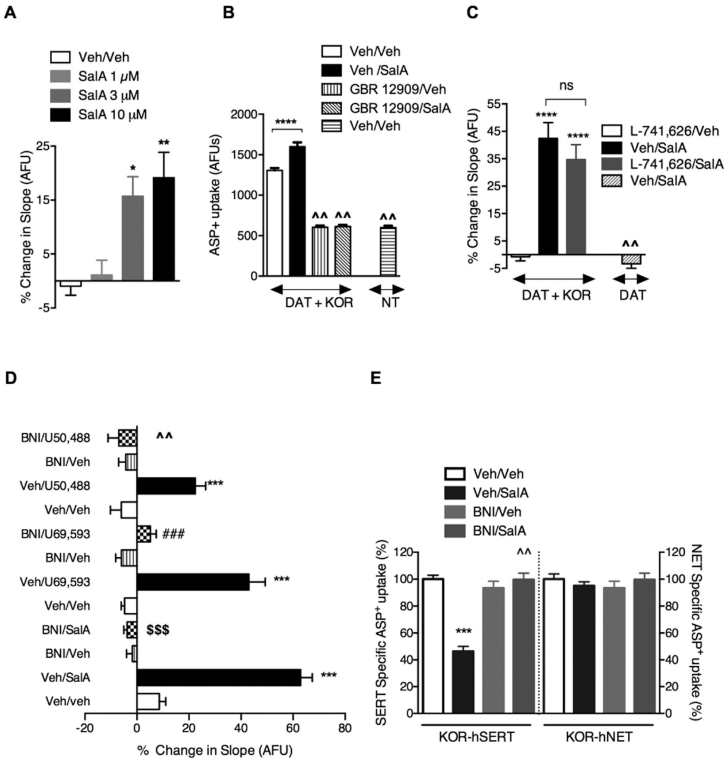

Fig. 1. SalA and other KOR agonists alter biogenic amine transporters function differentially via a BNI–reversible mechanism

EM4 cells were transiently cotransfected with myc-KOR plus YFP-DAT or myc-KOR plus hSERT or myc-KOR plus hNET. After 48 h, DAT, SERT and NET functions were measured as accumulation of ASP^+ over time as described under *Materials and Methods*. A. Influence of SalA concentrations (1 – 10 μM) on ASP^+ accumulation rate (AFU). *p< 0.05; **p < 0.001, (SalA 3 μM: n=47 and 10 μM: n=37 respectively) compared with vehicle control (One-Way ANOVA with Dunnett's multiple comparison test. B. Effect of DAT blocker GBR12909 on DAT mediated ASP^+ accumulation. GBR12909 (10 μM) blocked DAT mediated ASP^+ accumulation both in the presence and absence of SalA. ****p< 0.0001 (SalA: n=73) compared to corresponding Veh/Veh control (N=31). ^^p< 0.01 (GBR12909/Veh: n=160; GBR12909/SalA: n=118 and nontransfected cells: N=144) compared with Veh/Veh or Veh/SalA. The GBR12909 insensitive background signals were similar to those observed in nontransfected cells. C. Effect of D_2 receptor antagonist L-741,626 on SalA induced increase in ASP^+ accumulation. L-741,626 (10 μM) did not alter SalA induced increase in ASP^+ accumulation in EM4 cells coexpressing DAT and KOR. **** p< 0.0001 compared with L-741,626/Veh (N=181). SalA failed to increase DAT-mediated ASP^+ accumulation in EM4 cells expressing DAT only. ^^p< 0.01 (N=157) compared with Veh/SalA (N=149) or L-741,626/SalA (N=181) in cells coexpressing both DAT and KOR. ns, non significant, p=0.84, (Veh/SalA versus L-741,626/SalA). D. Effect of KOR agonists SalA (10 μM), U69,593 (10 μM) and U50,488 (10 μM) on DAT function. BNI (1 μM) prevents KOR evoked DAT upregulation. ***p< 0.001 (SalA: n=64; U69,593: n=35 and U50,488: n=55) versus corresponding Veh/Veh control; $^{\$\$\$}$p< 0.001 (n=60)

versus Veh/SalA; ###p< 0.001 (n=42) versus Veh/U69,593 and ^^p< 0.001 (n=44) versus Veh/U50,488. E. Effect of SalA (10 μM, 10 min) on SERT and NET function. A between cell design was utilized to determine the effect of SalA. Background uptake values were corrected and normalized to SERT or NET expression levels. ***p< 0.001 (n=47); significantly different from Veh/Veh control; ^^p< 0.01 (n=16) significant different compared with Veh/SalA. Data are the mean ± S.E.M (One-Way ANOVA with Bonferroni multiple comparison test).

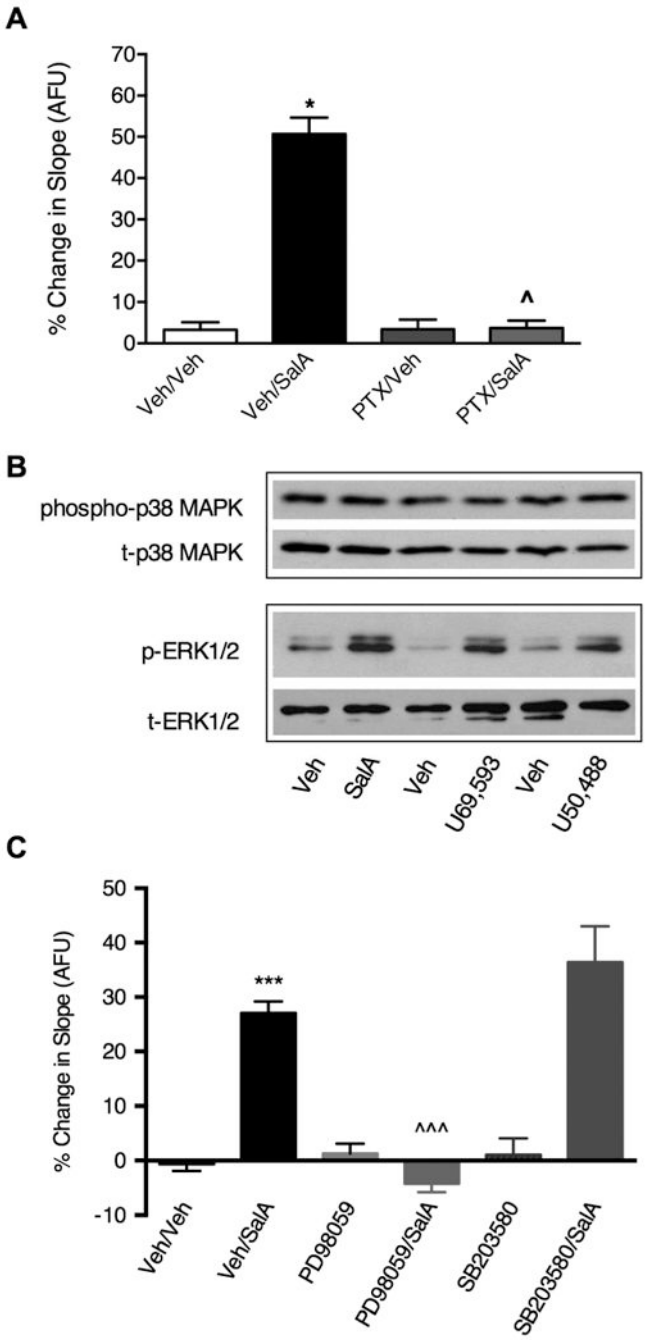

Fig. 2. SalA upregulates DAT function in PTX sensitive and ERK1/2-dependent mechanism

EM4 cells co-expressing myc-KOR and YFP-DAT were pre-incubated with PTX (100 ng/ml-16-24 hr) or PD98059 (10 μM-15 min) or vehicle prior to SalA (0; 10 μM) addition. ASP^+ uptake or t-ERK1/2 and p-ERK1/2 or phospho-p38 MAPK and t-p38 MAPK levels were determined as described under *Materials and Methods*. A. PTX pretreatment prevents SalA - evoked DAT upregulation. *$p< 0.01$ ($n=87$); significantly different from Veh/Veh control; ^$p< 0.01$ ($n=64$) significant difference compared with Veh/SalA (One-Way ANOVA with Bonferroni multiple comparison test). B. Representative immunoblot showing

phospho-ERK1/2, total ERK1/2, phospho-p38 MAPK and total p38 MAPK levels in vehicle or SalA or U69,593 or U50,488 treated cells. C. Pre-treatment of ERK1/2 inhibitor PD98059 but not p38 MAPK inhibitor SB203580 prevents SalA – induced DAT activity. ***$p < 0.001$ (n=89); significantly different from Veh/Veh control; ^^^$p < 0.001$ (n=71) significant difference compared with Veh/SalA. Data are the mean ± S.E.M (One-Way ANOVA with Bonferroni multiple comparison test). D. Representative immunoblot showing phospho-ERK1/2, total ERK1/2, phospho-p38 MAPK and total p38 MAPK levels in vehicle or SalA or PD98059 or PD98059/SalA treated cells.

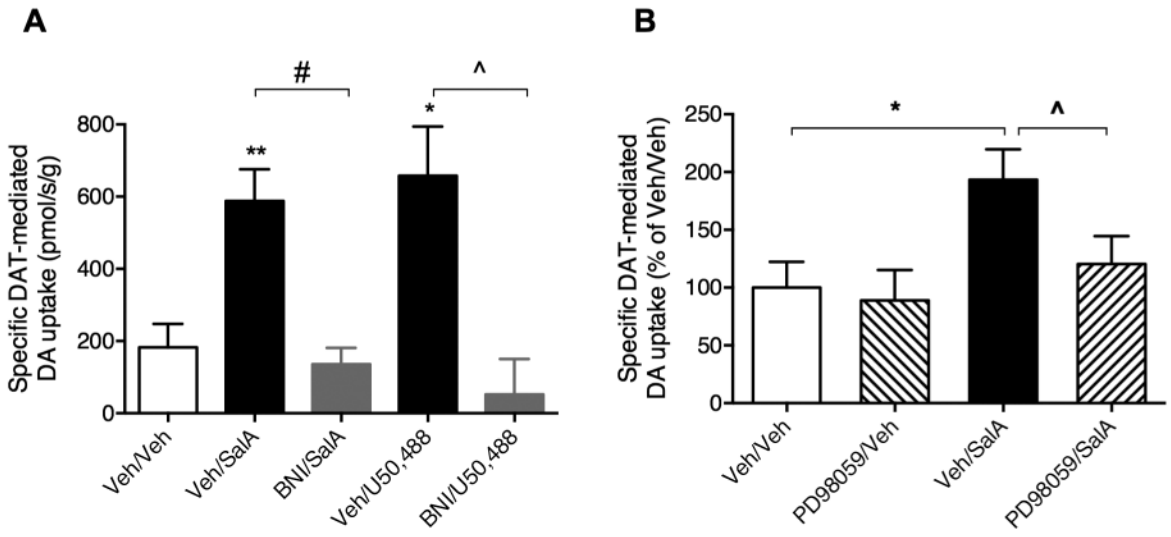

Fig. 3. KOR activation by SalA and U50,488 increases DA clearance in striatum and SalA-mediated DAT upregulation is ERK1/2 dependent

Minced slice preparations from rat striatum were exposed to appropriate vehicle(s) or SalA or U50,488 and RDE voltammetry was performed to measure DA clearance as described under *Materials and Methods*. GBR12909 (100 nM) was used to determine the specific DAT mediated DA clearance in RDE experiments. DA uptake in the presence of GBR12909 was subtracted from the total clearance to yield specific DAT-mediated DA uptake. A. KOR antagonist BNI blocked SalA (10 μM) or U50,488 (10 μM) induced DAT-mediated DA clearance. Slices were pre-incubated with BNI (1 μM-5 min) prior to SalA or U50,488 (0; 10 μM) addition. Values (pmoles/s/g tissue) represent the mean ± SEM of three independent experiments. *$p < 0.05$; **$p < 0.01$ compared with Veh/Veh control. #$p < 0.05$ compared with Veh/SalA. ^$p < 0.05$ compared with Veh/U50,488. (One-Way ANOVA with Bonferroni multiple comparison test). B. ERK1/2 inhibitor PD98059 prevents SalA induced changes in dopamine clearance. Minced slice preparations from rat striatum were exposed to vehicle or PD98059 (10 μM) for 10 min prior to the addition of SalA (0; 10 μM). RDE voltammetry was performed to measure DA clearance as described under *Materials and Methods*. Values were expressed as percentage of uptake relative to the uptake observed in Veh/Veh treated slices and represent the mean ± SEM of three independent experiments. *$p < 0.01$ significant difference between Veh/Veh *versus* Veh/SalA; ^$p < 0.04$ significant difference between Veh/SalA and PD98059/SalA (One-Way ANOVA with Bonferroni multiple comparison test).

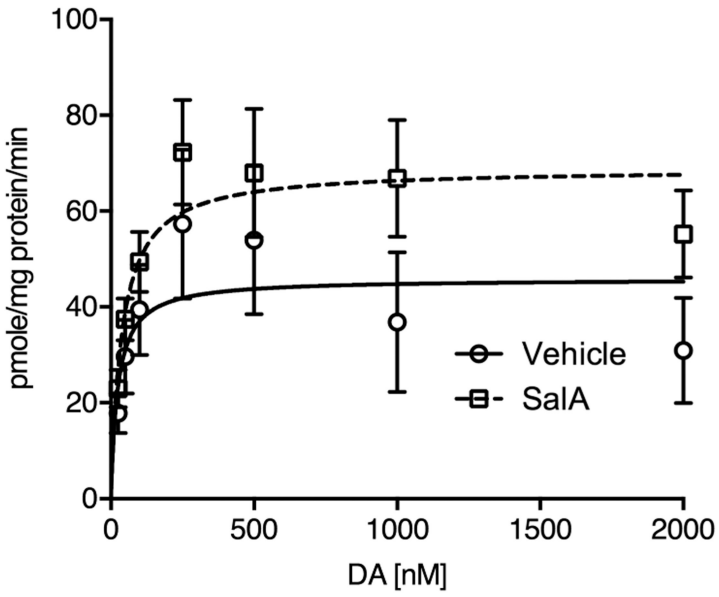

Fig. 4. SalA increases DAT V_{max}

DA uptake kinetic characteristics mediated by DAT in vehicle or SalA treated striatal synaptosomes. Synaptosomes (50 μg) were preincubated with the vehicle or SalA (10 μM) for 5 min at 37°C. After this treatment, uptake of DA was measured (5 min) over a range of 0.01 to 2 μM mixed with 50 nM nisoxetine (to block NET mediated DA uptake) and radiolabelled [^{3}H]DA as described under *Materials and Methods*. In parallel, nonspecific uptake at each concentration of DA used (in the presence of 100 μM cocaine) was subtracted from total uptake. Values are the averages from three independent experiments, and the mean values ± SEM are given. Nonlinear curve fits of data for uptake used the generalized Michaelis–Menten equation (Prism).

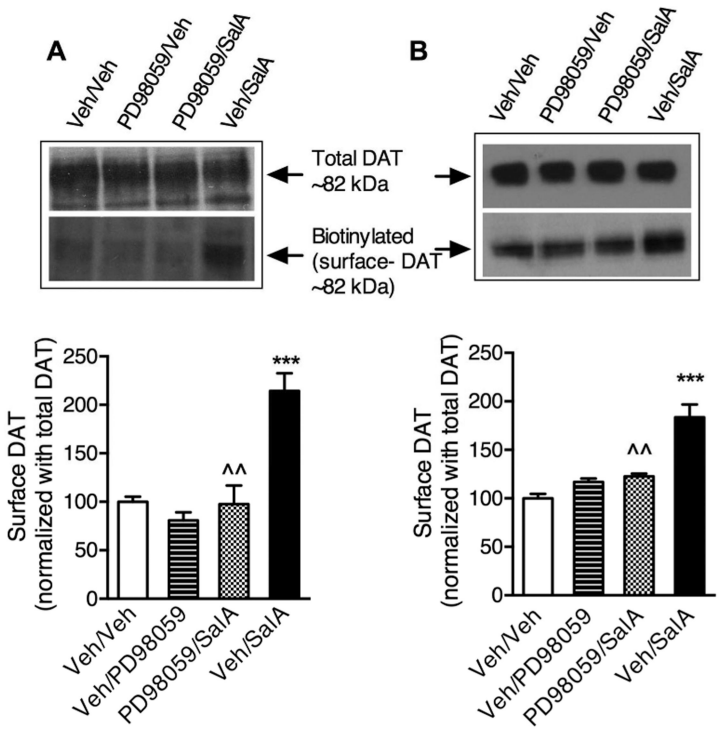

Fig. 5. SalA increases DAT cell surface expression and is ERK1/2 dependent

EM4 cells coexpressing myc-KOR and YFP-DAT or rat striatal synaptosomes were pre-treated with vehicle or PD98059 (10 μM) for 15 min prior to SalA (0; 10 μM, 5 min) followed by biotinylation. Isolation of biotinylated proteins, detection and quantification of DAT were performed as described under *Materials and Methods*. Western blots of DAT from total lysates and avidin bead eluates from striatal synaptosomes (A) and EM4 cells coexpressing KOR and DAT (B) are shown at the top. Quantified surface DAT band densities are shown at the bottom. *** $p<0.001$ (N=9) significant changes in biotinylated DAT band densities compared with Veh/Veh control (n=8) or Veh/PD98059 (N=4) or PD98059/SalA (N=9) in EM4 cells and striatal synaptosomes (Veh/Veh control (n=11) or Veh/PD98059 (N=3) or PD98059/SalA (N=3). ^^$p<0.005$ (Veh/Sal versus PD98509/SalA). Data are the mean ± S.E.M (One-Way ANOVA with Bonferroni multiple comparison test).

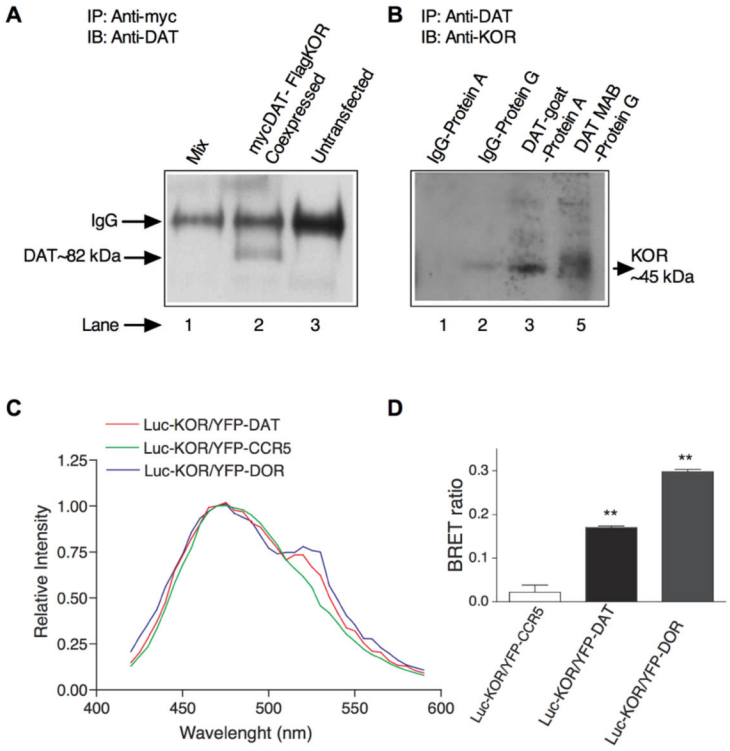

Fig. 6. Presence of DAT and KOR as an oligomerization complex

A. Co-immunoprecipitation of KOR and DAT from EM4 cells transfected with myc-KOR or Flag-DAT. Lane 1: Lysates from EM4 cells individually expressing myc-KOR or Flag-DAT were mixed; immunoprecipitated (IP) with an anti-myc antibody and immunobloted (IB) using an anti-DAT antibody. Lane 2: Lysates from EM4 cells coexpressing myc-KOR and Flag-DAT were immunoprecipitated and immunobloted as described in lane 1. Lane 3: non-transfected cells. A representative blot of n=5 experiments is shown. IgG bands were detected due to the presence of IgG in eluate from immunocomplex and due to the cross immunoreactivity of secondary antibody. B. Co-immunoprecipitation of DAT from rat striatal synaptosomes. The synaptosomes were solubilized and immunoprecipitated using two different DAT antibodies. Parallel experiments using irrelevant IgG were performed to validate the specificity of immunoprecipitation. Presence of KOR from DAT-immunocomplex was determined by immunoblotting with KOR antibody as described under *Materials and Methods*. The experiment shown was replicated with similar results and representative immunoblot is shown. C. BRET: KOR and DAT are in close proximity. HEK cells were transfected as described in Methods and subjected to BRET analysis. Light emission spectra for the conditions are shown. D shows the BRET ratios determined from light emission spectra. **p<0.01.

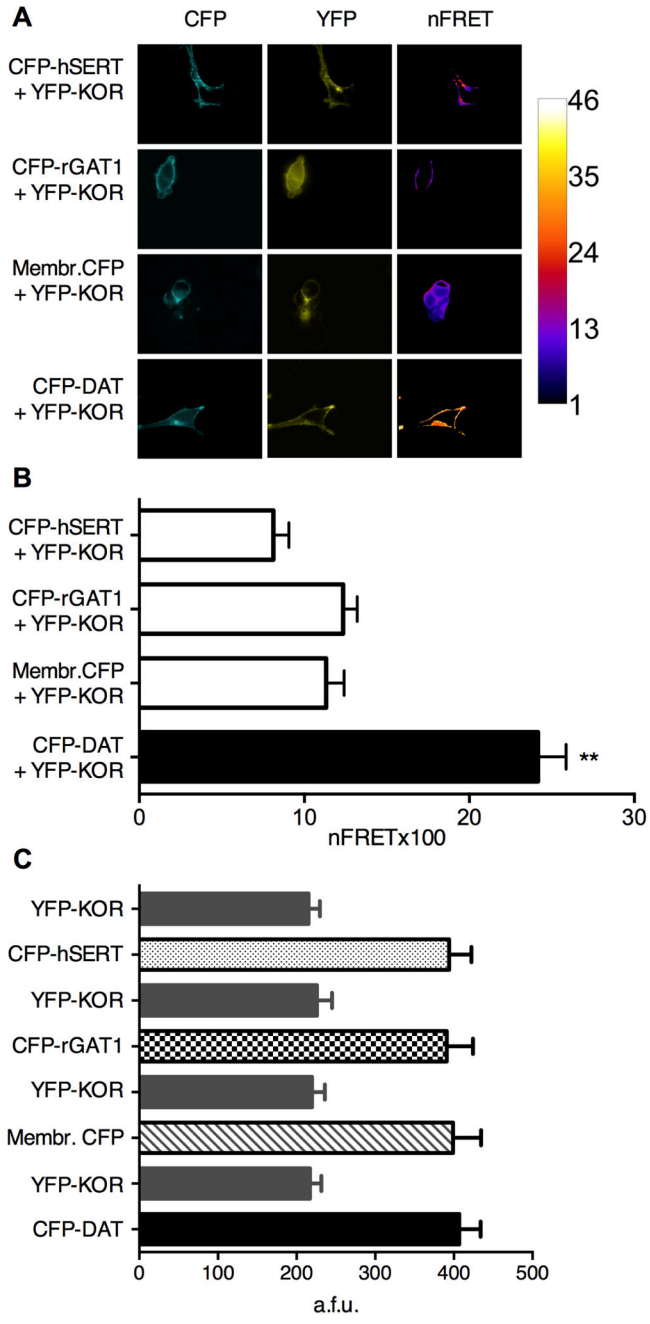

Fig. 7. FRET Analysis of DAT and KOR oligomerization in Living Cells

FRET microscopy showed the presence of DAT and KOR oligomerization in DAT and KOR coexpressing intact cells as described under *Materials and Methods*. A. HEK293 cells were cotransfected with YFP-KOR and CFP-tagged other cDNAs as given in the figure. 48 h post transfections, epifluorescence microscopy was performed in live cells. Images from the filter sets, CFP (first column), YFP (second column) and corrected and normalized FRET (nFRET) images (third column) are shown. A color code used is also presented on the right corner of the figure. Background fluorescence was subtracted from all images

presented. B. Normalized FRET efficiencies are given from cells coexpressing CFP-DAT + YFP-KOR (n=33); membr.CFP + YFP-KOR (n=27); CFP-GAT1 + YFP-KOR (n=27) and CFP-hSERT + YFP-KOR (n=27). **Significant difference between CFP-DAT + YFP-KOR and membr.CFP + YFP-KOR ($p<0.0001$) or CFP-DAT + YFP-KOR and CFP-GAT1 + YFP-KOR ($p<0.0001$) or CFP-DAT + YFP-KOR and CFP-hSERT + YFP-KOR ($p<0.0001$). C. Expression levels of CFP-DAT, Membr-CFP, CFP-GAT1, CFP-SERT and YFP-KOR. Intensity of fluorescence was measured in a 1 pixel-broad rim positioned over the membrane. Values were expressed as arbitrary fluorescence units (a.f.u.). Data were analysed using One-way ANOVA with Bonferroni's multiple comparisons test.

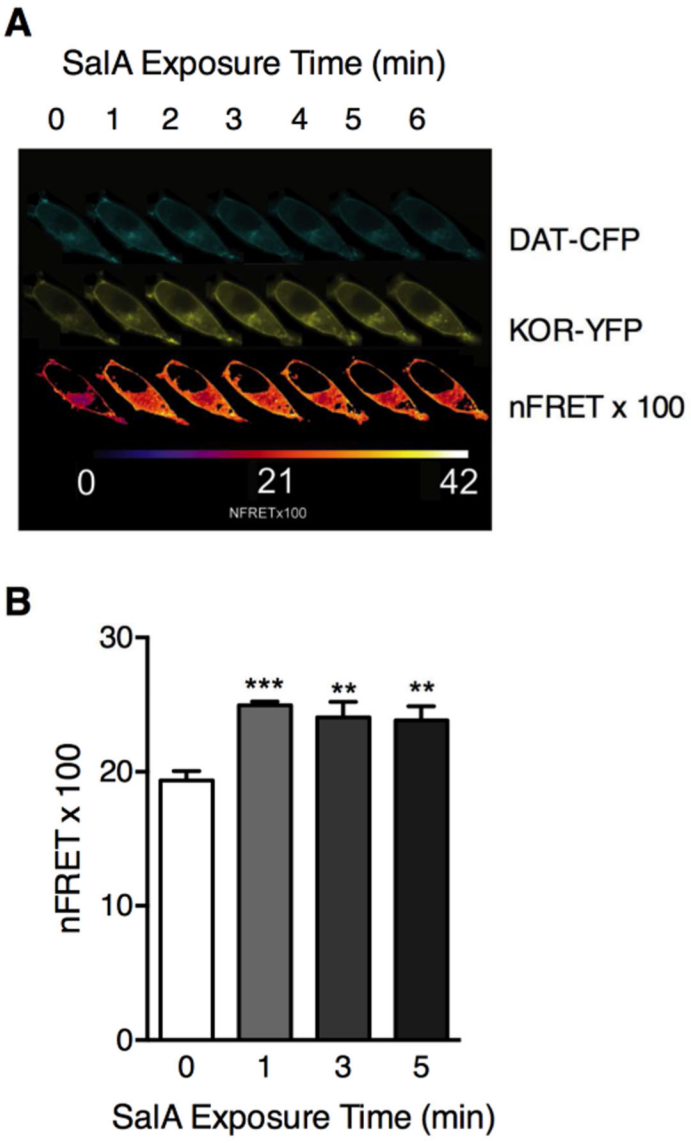

Fig. 8. SalA treatment increases DAT and KOR oligomerization

HEK293 cells coexpressing DAT-CFP + YFP-KOR were exposed to SalA (10 μM) for various times (0 to 6 min) followed by FRET analysis as described in Fig. 6 and under *Materials and Methods*. A. Images obtained at different time periods using different filter sets, DAT-CFP (first row from the top), YFP-KOR (second row from the top) and corrected and normalized FRET (nFRET) images (third row from the top) and the color code are shown. B. Normalized FRET efficiencies for each time points are given. **Significant difference between 0 and 1 min ($p<0.001$, n= 4), 0 and 3 min ($p<0.005$, n= 4) and 0 and 5 min ($p<0.008$, n= 4). Data were analysed using One-way ANOVA with Bonferroni's multiple comparisons test.